

**2012 Bachelor Thesis**

**Conduction Mechanism at Low Temperature of  
2-Dimensional Hole Gas at  
GaN/AlGaN Heterointerface**  
(低温における GaN/AlGaN ヘテロ界面の  
2次元正孔ガスの伝導機構)

**Supervisor: Prof. Hiroshi Iwai**

**Supervisor: Associate Prof. Kuniyuki Kakushima**

**Tokyo Institute of Technology**

**Department of Electrical and Electronic Engineering**

**09\_26341 Pucheng Liu**

<b>Supervisor Seal</b>	
------------------------	--

<b>Department Chairman Seal</b>	
---------------------------------	--

February, 2013

Abstract of Bachelor Thesis

## **Conduction Mechanism at Low Temperature of 2-Dimensional Hole Gas at GaN/AlGa<sub>N</sub> Heterointerface**

Supervisor: Prof. Hiroshi Iwai

Assistant Prof. Kuniyuki Kakushima

Department of Electrical and Electronic Engineering

09\_26341 Liu Pucheng

Since the GaN-based heterostructure field-effect transistors (HFETs) have demonstrated high RF output power levels, it is treated as a candidate promising candidates to realize high power integrated circuits. N-channel type GaN devices such as High High Electron Mobility Transistors, is under research mostly, and some of them have already been commercialized. In order to produce logic cuircuts likely to Si-based CMOS technologies, p-channel GaN materials are considered fatal to the development of next generation power integrated circuit using GaN. To avoid the problems that the Mg doped p-type GaN has a limited activation ratio and difficult to obtain high mobility and carrier density enough, the polarization at GaN/AlGa<sub>N</sub> heterointerface is used in this research.

In this article, a sample made from GaN/AlGa<sub>N</sub>/GaN heterostructure is presented. 2-D hole gas (2DHG) is generated by negative polarization at the upper GaN/AlGa<sub>N</sub> interfaces. Metal electrodes are added to the upper surface of GaN/AlGa<sub>N</sub>/GaN heterostructure to measure electrical properties of the 2DHG. In order to obtain a non-rectifying property at the metal/GaN interface, wet chemical etching and heat treatment are performed. Firstly several conditions of wet chemical etching and heat treatment were tested and then samples of Hall effect measurements were fabricated at the optimum process condition. Van der Pauw method of Hall measurement was used in this experiment and the dependence of mobility, sheet resistance, sheet carrier density and temperature was obtained in a range of 80-460 K.

A totally different electrical property especially in the low temperature less than 200 K, is observed in the experiment for polarized GaN/AlGa<sub>N</sub>/GaN heterostructure compared with conventional Mg-doped GaN. The measured results indicate that a p-type conduction mechanism in polarized GaN/AlGa<sub>N</sub>/GaN is a “band conduction” in low temperature. A possible reason for the difference is given in this article.

# Contents

<b>Chapter 1. Introduction.....</b>	<b>5</b>
1.1 Metal-Oxide-Semiconductor Field-Effect Transistor and Heterojunction Field-Effect Transistor .....	6
1.2 Gallium Nitride .....	7
1.3 2-Dimensional Hole Gas (2DHG) .....	9
1.4 Electrical Properties of 2DHG HFET .....	10
1.5 Conduction Mechanism of 2DHG .....	10
1.6 Toward Future Research .....	10
Reference .....	11
<b><u>Chapter 2. Equipment and Techniques.....</u></b>	<b>12</b>
2.1 Transmission Electron Microscope (TEM) .....	13
2.2 Secondary Ion Mass Spectrometry (SIMS) .....	13
2.3 Hall Effect Measurement .....	14
2.3.1 Hall Effect .....	14
2.3.2 Hall Effect Measurement .....	16
2.3.2.1 Conditions of the Samples .....	16
2.3.2.2 Necessary Conditions for the Contacts: Non-Rectifying .....	16
2.3.2.3 Measurement of Resistance .....	18
2.3.2.4 Measurement of Sheet Carrier Density and Mobility .....	19
2.3.3 Equipment for Hall Effect .....	20
2.4 Rapid Thermal Annealing (RTA) .....	22
2.5 Probe Station .....	23
2.6 Photolithograph .....	24

Reference .....	27
<b><u>Chapter 3. Experimental Procedures</u></b> .....	<b>28</b>
3.1 Procedures Needed for the Research .....	29
3.2 Preprocessing .....	29
3.2.1 Methods for Preprocessing .....	29
3.2.2 Most Suitable Method for Preprocessing .....	30
3.3 Steps of Experiment .....	33
Reference .....	35
<b><u>Chapter 4. Results</u></b> .....	<b>36</b>
4.1 TEM .....	37
4.2 SIMS .....	38
4.3 Dependence of sheet carrier density, sheet resistance and mobility on temperature .....	39
<b><u>Chapter 5. Conclusion</u></b> .....	<b>42</b>
5.1 Conduction Mechanism of Mg-doped GaN .....	43
5.1.1 Band Conduction .....	43
5.1.2 Impurity-band Conduction .....	47
5.1.3 Hopping Conduction .....	47
5.2 Conduction Mechanism of AlGa <sub>N</sub> /Ga <sub>N</sub> Heterointerface .....	48
Reference .....	50
<b><u>Acknowledgement</u></b> .....	<b>51</b>

# **Chapter 1: Introduction**

<b>1.1</b> Metal-Oxide-Semiconductor Field-Effect Transistor and Heterojunction Field-Effect Transistor .....	6
<b>1.2</b> Gallium Nitride .....	7
<b>1.3</b> 2-Dimensional Hole Gas (2DHG) .....	9
<b>1.4</b> Electrical Properties of 2DHG HFET .....	10
<b>1.5</b> Conduction Mechanism of 2DHG .....	10
<b>1.6</b> Toward Future Research .....	10
Reference .....	11

## 1.1 Metal-Oxide-Semiconductor Field-Effect Transistor and Heterojunction Field-Effect Transistor

As a fundamental element in electronics industry, transistor plays an important role. In the design of transistor, to reduce the resistance is important considering the loss of signal.

Metal-Oxide-Semiconductor Field-Effect Transistor (MOSFET) is one of most commonly used transistors.

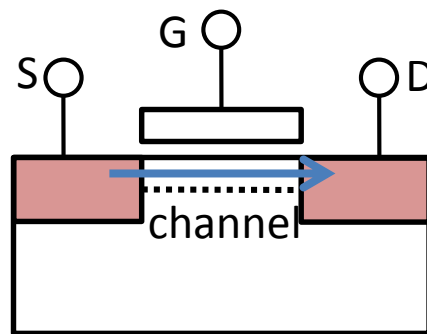


**Fig1.1 Structure of MOSFET**

As shown in Fig 1.1, the voltage from Gate (G) leads to a channel developed between source (S) and drain (D), and the carrier can transverse through the channel.

Compared to MOSFET, heterojunction field effect transistors (HFETs) develop a channel by a junction between two materials with different band gaps.

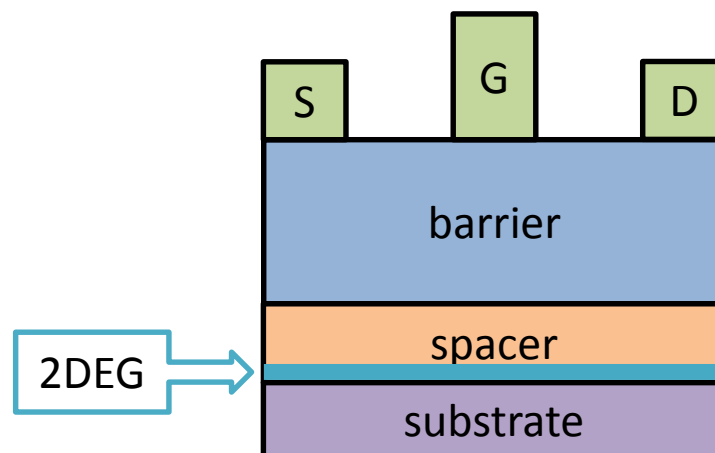


**Fig1.2 Structure of HFET**

As shown in Fig 1.2, the difference of the band of the spacer and the substrate leads to a quantum well, an uncontinuous area of the band. As a result, the carrier will assume at

the interface. If the carrier is electron rather than hole we call this layer two dimensional electron gas (2DEG).

As shown in Fig 1.3, the quantum well leads to an area where the Fermi level is higher than the edge of conduction band. This develops the two dimensional electron gas.

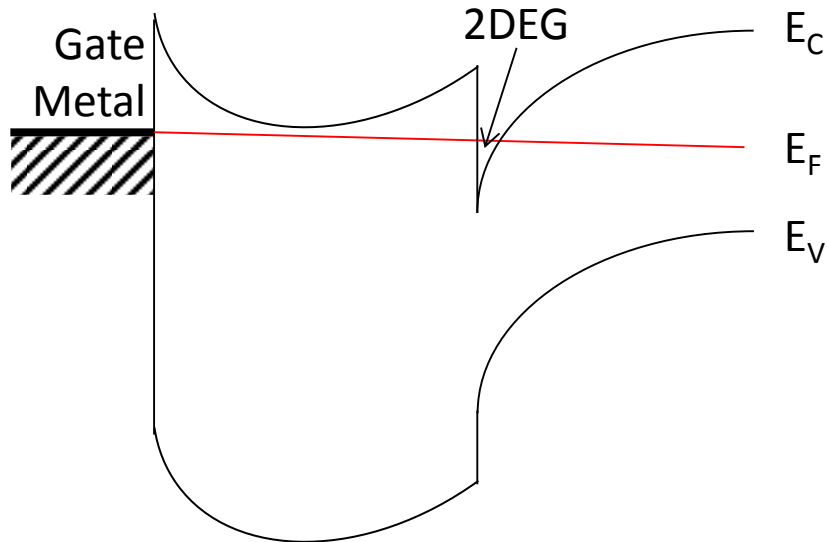


**Fig 1.3 Band Structure in HFET**

As mentioned at the beginning, to obtain relatively low resistance is important in VLSI industry. As known, the electrical resistivity can be written as

$$\rho = \frac{1}{qn\mu} \quad (1.1)$$

$q$  is the charge on the particle;  $n$  is the majority carrier density;  $\mu$  is the mobility of the carrier.

From (2.1), we know that the resistivity can be reduced by increasing the carrier density. But for increasing the carrier density will lead to decrease in mobility, to have low resistivity only by increasing the carrier density is difficult. To obtain both high carrier density and high mobility is important, but it is hard to realize in traditional MOSFET structure.

In HEFT structure, as the material use in spacer is undoped, so the influence by impurity scattering is less. As a result, both high carrier density and high mobility can be realized in this structure.

## 1.2 Gallium Nitride

Gallium nitride (Molecular formula: GaN) is a kind of III-V component and has been being used in semiconductor industry since the 1990s, especially LED. The electrical

properties of gallium nitride and other semiconductor materials are shown in Table 1.1. [1]

**Table 1.1 Physical Properties of Semiconductor Materials**

	Si	GaAs	4H-SiC	GaN
Band Gap [eV]	1.1	1.4	3.3	3.4
Breakdown Voltage [MV/cm]	0.3	0.4	3.0	3.3
Saturated Electron Velocity [ $10^7$ cm/s]	1.0	2.0	2.0	2.5
Electron Mobility [ $\text{cm}^2/\text{Vs}$ ]	1500	8500	1000	1200
Hole Mobility [ $\text{cm}^2/\text{Vs}$ ]	600	400	115	~10
Coefficient of Thermal Conductivity [W/cmK]	1.5	0.5	4.9	2.1

As shown in Table 1.1, the band gap of gallium nitride, which is nearly equal to that of silicon carbide, is 3 times as silicon. On-resistance of gallium nitride device is thought one third of silicon device, for the breakdown voltage of gallium nitride is 3 times higher than silicon.

Gallium nitride has a Wurtzite crystal structure. Wurtzite crystal structure is an example of hexagonal crystal system, and often seen in the structure of zinc sulfide (ZnS). The structure of gallium nitride is shown in Fig 1.4. [2]

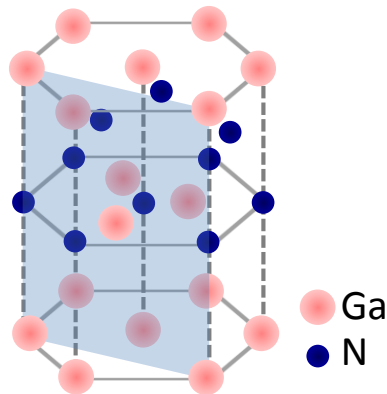


**Fig 1.4 Structure of Gallium Nitride**

Compared to silicon carbide, a great advantage of gallium nitride is, that GaN has relatively large discontinuity in bandgap with materials such as AlGaN, so it can be used to form good heterojunction structure.

Another reason why GaN is chosen as the experimental material, is that the manufacture of SiC, is limited. This material is somehow difficult to obtain nowadays.



### 1.3 2-Dimensional Hole Gas (2DHG)

The electrical characters of HFETs with two dimensional electron gas (2DEG) have been reported in several articles. It is reported that high density 2DEG can be obtained by using positive polarization charges at the AlGa<sub>0.23</sub>Ga<sub>0.77</sub>N/GaN interface. Therefore, the 2DEG mobility is as high as 1000cm<sup>2</sup>/Vs, so it is treated as important candidate for next generation power device.

Similar with 2DEG, two dimensional hole gas (2DHG) has been predicted in several articles, but reports in which 2DHG is observed are few. According to the prediction, 2DHG should have properties as high mobility and high density.

In this experiment, we demonstrated a p-channel HFETs using GaN/AlGa<sub>0.23</sub>Ga<sub>0.77</sub>N/GaN heterostructure. The basic structure of the sample used in this research is shown as Fig 1.5. As shown in this figure, 2DHG exists at the upper GaN/AlGa<sub>0.23</sub>Ga<sub>0.77</sub>N interface, and 2DEG exists at the lower AlGa<sub>0.23</sub>Ga<sub>0.77</sub>N/GaN interface.

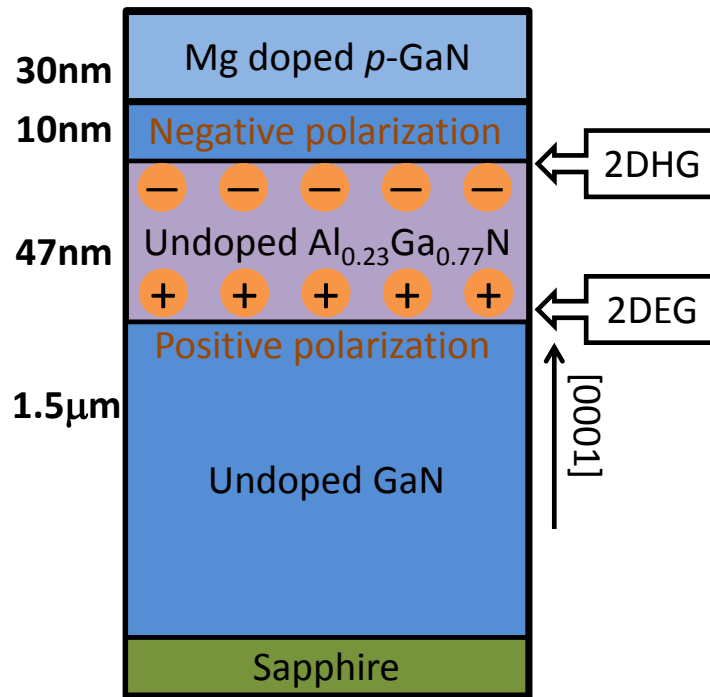


Fig 1.5 Structure of Sample

As only 2DEG is used in traditional HFET due to the high resistivity of 2DHG, CMOS circuit cannot be realized in HFET. In order to produce circuits CMOS contained, it is necessary to develop low resistance 2DHG. For illustration, Electric power conversion machine is considered can be modified to a one-chip circuit using the GaN-Based CMOS. High breakdown voltage is fatal to this kind of power device and GaN can satisfy it.

## **1.4 Electrical Properties of 2DHG HFET**

According to A. Özgür *et al*, using positive polarization charges at the AlGa<sub>N</sub>/Ga<sub>N</sub> interface leads to high density 2DEG with the densities over  $10^{13}$  cm<sup>-2</sup> can be obtained. [3,4] In this research, a sheet carrier density of AlGa<sub>N</sub>/Ga<sub>N</sub> interface of about  $1.8 \times 10^{13}$  cm<sup>-2</sup> at room temperature has been confirmed. The detailed will be reported in Chapter 4.

## **1.5 Conduction Mechanism of 2DHG**

From the results of these experiments, we consider the conduction mechanism. Due to the limited experiment equipment, we cannot give a precise answer about the conduction mechanism, but a possible mechanism is given in Chapter 5.

## **1.6 Toward Future Research**

The sample produced in this research has a sheet carrier density and mobility enough to manufacture CMOS circuit combined with 2-Dimensional Electron Gas according to the prediction.

## Reference

- [1] M.Hikita, M.Yanagihara, Y.Uemoto, T.Ueda, T.Tanaka and D.Ueda, 2009, “GaN-based power Devices”, *Panasonic Technical Journal*, **55**, 92-95
- [2] B. Monemar and Pozina, “Group III-nitride based hetero and quantum structures”, 2000, *Progress in Quantum Electronics*, **24**, 239-290
- [3] A. Özgür, W. Kim, Z. Fan, A. Botchkarev, A. Salvador, S.N. Mohammad, B. Sverdlov and H. Morkoç, 1995, “High transconductance-normally-off GaN MODFETs”, *Electronic Letters*, **31**, 1389-1390
- [4] O. Ambacher, J. Smart, J. R. Shealy, N. G. Weimann, K. Chu, M. Murphy, W. J. Schaff, L. F. Eastman, R. Dimitrov, L. Wittmer, M. Stutzmann, W. Rieger, and J. Hilsenbeck, 1999, *Journal of Applied Physics*, **85**, 3222-3233

## **Chapter 2: Equipment and Techniques**

<b>2.1</b>	Transmission Electron Microscope (TEM) .....	13
<b>2.2</b>	Secondary Ion Mass Spectrometry (SIMS) .....	13
<b>2.3</b>	Hall Effect Measurement .....	14
<b>2.3.1</b>	Hall Effect .....	14
<b>2.3.2</b>	Hall Effect Measurement .....	16
<b>2.3.2.1</b>	Conditions of the Samples .....	16
<b>2.3.2.2</b>	Necessary Conditions for the Contacts: Non-Rectifying .....	16
<b>2.3.2.3</b>	Measurement of Resistance .....	18
<b>2.3.2.4</b>	Measurement of Sheet Carrier Density and Mobility .....	19
<b>2.3.3</b>	Equipment for Hall Effect .....	20
<b>2.4</b>	Rapid Thermal Annealing (RTA) .....	22
<b>2.5</b>	Probe Station .....	23
<b>2.6</b>	Photolithograph .....	24
	Reference .....	27

## 2.1 Transmission Electron Microscope (TEM)

Transmission Electron Microscope is a kind of microscope, which is often used to observe the structure of ultra-thin semiconductor materials. It is important equipment in not only electronics but also in other fields like biology. [1]

In transmission electron microscopy technique, electrons from an electron gun will transmit through the specimen, and the image of the specimen will be formed from the information obtained through the interaction of the electrons and specimen.

Resolve detail in an object was limited approximately by the wavelength of the light used in imaging. In optical microscopy technique, it is hard to observe specimens under a few hundred nanometers for this reason. Let  $\lambda$  be the wavelength of photons, and  $NA$  be the numerical aperture of the system, so the maximum resolution is

$$d \approx \frac{\lambda}{2NA} \quad (2.1)$$

For the small de Broglie wavelength of electrons, the TEM has a resolve detail about tens of thousands times better than optical microscope. Considering the relativity, the de Broglie wavelength of electron is

$$\lambda_e \approx \frac{h}{\sqrt{2m_0E(1 + \frac{E}{2m_0c^2})}} \quad (2.2)$$

$h$  is Planck's constant,  $m_0$  is the rest mass of an electron and  $E$  is the energy of the accelerated electron. Highly accelerated electrons lead to high resolution. The electron beam will transmit through the specimen and then contains the information of electron density, phase and periodicity. The information will be analyzed and used to form the image of the specimen. Let  $\Psi$  be the wave function of the electron transmitted from the specimen, so the observed intensity of the image is

$$I(x) = \frac{k}{t_1 - t_0} \int_{t_0}^{t_1} \Psi\Psi^* dt \quad (2.3)$$

## 2.2 Secondary Ion Mass Spectrometry (SIMS)

The secondary ion mass spectrometry (SIMS) is a technique used to analyze the

composition of the material. The model of SIMS is shown schematically in Fig 2.1.

Primary ions (usually Cs<sup>+</sup> or O<sub>2</sub><sup>+</sup>) are accelerated to high speed with a kinetic energy of about 10kV by an ion gun. The primary ions will sputter the surface of the specimen and the secondary ions will eject from the specimen. Then analyzers of the machine will collect information such as the type and the mass of the secondary ions. Through the SIMS measurement, we can obtain the dependence of the concentration of the elements and depth.

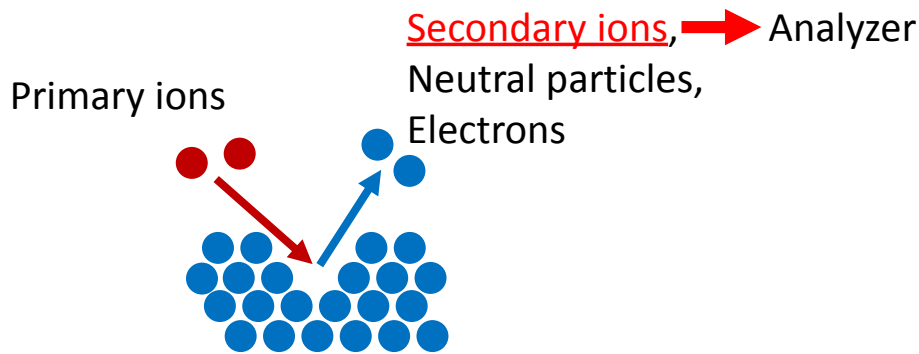


Fig 2.1 The Model of Secondary Ion Mass Spectrometry

## 2.3 Hall Effect Measurement

### 2.3.1 Hall Effect

The Hall Effect is a phenomenon in which a conductor or semiconductor that carries an electric current perpendicular to an applied magnetic field develops a voltage gradient transverse to both current and field. The voltage is known as the Hall voltage.

Consider the sample shown in Fig 2.2 has height, width, depth  $a, b, d$ , and the current flows through the plane  $ad$ , and the magnetic field is parallel to the plane  $ad$ .

Under this situation, the Lorentz force is

$$F_L = qvB \quad (2.4)$$

$q$  is the electrical charge on the particle;  $v$  is the velocity of the particle;  $B$  is the strength of the magnetic field.

The current which flows through the plane can be written as

$$I = qvnad \quad (2.5)$$

where  $n$  is the carrier density.

So we have

$$v = \frac{I}{qnad} \quad (2.6)$$

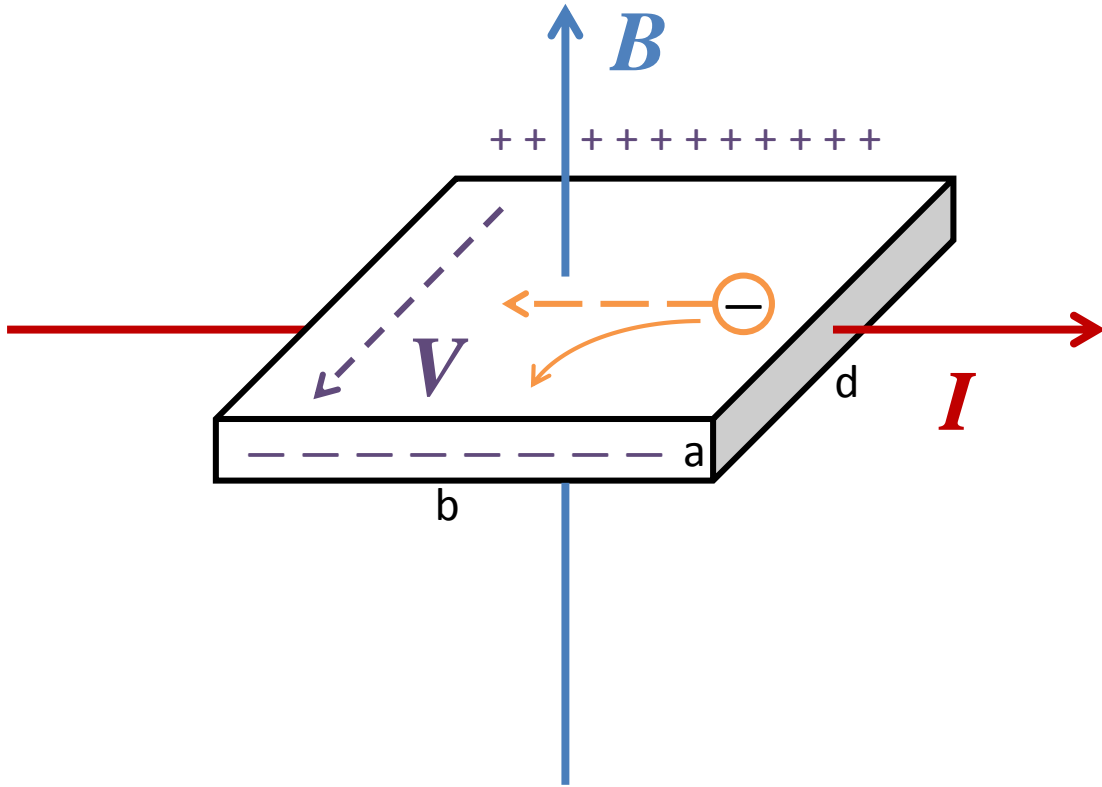


**Fig 2.2 Hall Effect**

From (2.4) and (2.6), we have

$$F_L = q \cdot \frac{I}{qnad} \cdot B = \frac{IB}{nad} \quad (2.7)$$

On the other hand, the voltage developed will lead to an electrical field, and this field will cause a force on the carrier, as

$$F_E = q \cdot \frac{V}{a} \quad (2.8)$$

where  $V$  is the voltage.

The Lorentz force balances the Coulomb's force, because the current continues to flow along the sample, so

$$\frac{IB}{nad} = q \cdot \frac{V}{a} \quad (2.9)$$

Hence

$$V = \frac{IB}{nqd} \quad (2.10)$$

Then we can rewrite (2.10) by sheet carrier density  $n_s$  as

$$V = \frac{IB}{n_s q} \quad (2.11)$$

It shows that we can know sheet carrier density by measuring the Hall voltage.

Therefore, as the direction of flow of current is depend on both the direction of the velocity of the move of the carriers and the type of the electric charge of the carriers, we can judge whether the carriers are holes or electrons by the polarization of the Hall voltage.

### **2.3.2 Hall Effect Measurement**

Van der Pauw method was used in this experiment in order to measure the properties of the samples. The van der Pauw method, which was first propounded by Leo J. van der Pauw in 1958, is a technique widely used in measure electrical properties of two-dimensional samples.

#### **2.3.2.1 Conditions of the Samples**

Firstly, the sample to be measured by the van der Pauw method should be two-dimensional; namely the samples should be of a flat shape of uniform thickness, and the sample should not have any isolated holes.

Although the van der Pauw method is designed for sample of arbitrary shape, it is found that the measurement error is smaller if using a homogeneous and isotropic sample. So it is better to make the sample homogeneous and isotropic.

In order to flow currency to the samples, we also need add contacts to the surface of samples. Four contacts are needs, and in order to minimize the measurement error, the contacts should be sufficiently small compared to the size of the sample, and be located at the edge of sample.

As discussed below, necessary conditions of sample for the measurement can be listed as:

- a) The sample must have a flat shape of uniform thickness.
- b) There are no isolated holes in the sample.
- c) The sample must be homogeneous and isotropic.
- d) Four contacts must be located at the edges of the sample.
- e) The area of contact of any individual contact should be small compared to the size of sample.

#### **2.3.2.2 Necessary Conditions for the Contacts: Non-Rectifying**

Another necessary condition for the contact is that the contacts should be ohmic. Namely, the contacts should be non-rectifying, which means that the current–voltage



curve of the region is linear and symmetric.

When metal and semiconductor are in contact, a barrier will exist between the two kinds of materials. The barrier is called Schottky Barrier (Fig 2.3). The Schottky Barrier prevents the move of the carrier between metal and semiconductor, so the contact becomes rectifying. This kind of rectifying behavior can be found in almost all metal-semiconductor contacts.

In measurement using van der Pauw method, the Schottky Barrier between metal contacts and semiconductor sample is treated as a problem. Basically we want an ohmic contact, which obeys Ohm's law. Some properties of the sample, such as resistance, cannot be measured correctly if the Schottky Barrier exists.

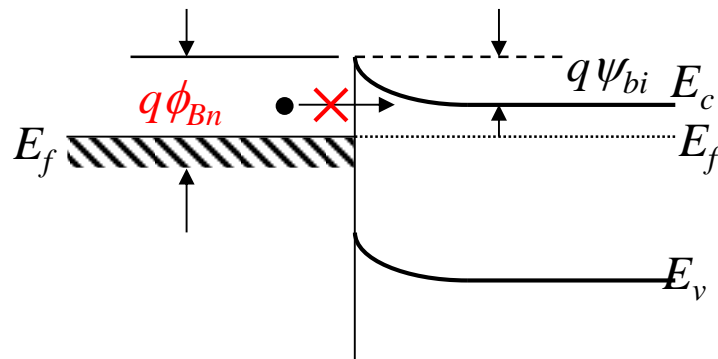


**Fig 2.3 Schottky Barrier**

Although totally removing the Schottky Barrier is treated impossible, there are two methods to make the Schottky contact look like an ohmic contact. Under such situation, where the current–voltage curve of the region approximates a linear function, we can obtain the correct signals out and into the sample.

The two ways to make metal-semiconductor contact ohmic are:

- a) Lower the Schottky Barrier Height(SBH)

As shown in (), The SBH is related to the work function of metal and the electron affinity.

$$\varphi_{SB} = \varphi_m - \chi \quad (2.12)$$

$\varphi_{SB}$  is the SBH;  $\varphi_m$  is the work function of metal;  $\chi$  is the electron affinity.

We can choose the proper metal, whose work function is nearly equal to the electron affinity of semiconductor which we use as sample, in order to lower the SBH.

Another method to lower the SBH is to create an alloy at the interface between metal and semiconductor, by heat treatment such as annealing, which is widely used.

- b) To create Quantum tunnelling

According to the theory of quantum mechanism, a particle, which behaves itself as

wave due to the wave–particle duality, is possible to tunnel through a barrier, through which it cannot tunnel under classic mechanism theory. If we can make the possibility to tunnel through the SBH high sufficiently to make the carrier move freely to both directions, we can make the metal–semiconductor contact ohmic. According to the mathematical analysis using the wave function in the Schrödinger equation, if SBH is extremely thin, the carrier will have relatively high possibility to tunnel through it. We can make the barrier very narrow by doping it very heavily, so the impurity concentration in the semiconductor is very important. Although change the impurity concentration is not easy considering other properties of the sample (e.g. the impurity concentration will effect on the mobility and resistance), we can make the impurity concentration near the surface between the two materials by heat treatment. By this method we can also obtain non-rectifying contact. [2]

### 2.3.2.3 Measurement of Resistance

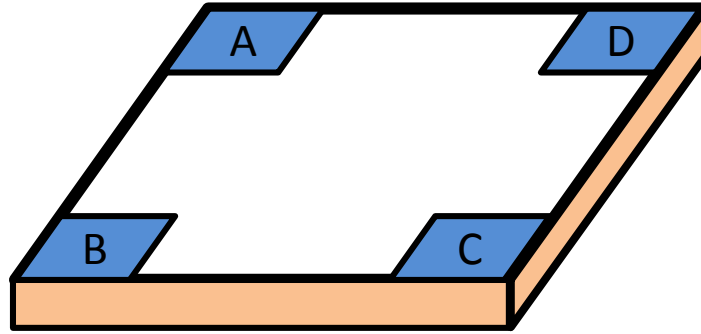


**Fig 2.4 Sample for Hall Measurement**

Let us consider a sample which satisfies the conditions mention in section 2.3.2.1, as shown in Fig 2.4. Four contacts are at the edges of a sample of sharp of square and named A, B, C, and D. If the current flows between contact A and B is defined as  $I_{AB}$  and the potential difference between D and C ( $V_D - V_C$ ) is  $V_{CD}$ .

Then we define  $R_{AB, CD}$  as:

$$R_{AB,CD} = \frac{V_{CD}}{I_{AB}} \quad (2.13)$$

Likely, we can define  $R_{BC, DA}$  as

$$R_{BC,DA} = \frac{V_{DA}}{I_{BC}} \quad (2.14)$$

$R_{AB, CD}$  and  $R_{BC, DA}$  can be shown that they follow:

$$\exp\left(-\pi \frac{R_{AB,CD}}{R_s}\right) + \exp\left(-\pi \frac{R_{BC,DA}}{R_s}\right) = 1 \quad (2.15)$$

$R_s$  is the sheet resistance, And it can be rewritten as:

$$R_s = \frac{\pi}{\ln 2} \frac{(R_{AB,CD} + R_{BC,DA})}{2} f \left( \frac{R_{AB,CD}}{R_{BC,DA}} \right) \quad (2.16)$$

where

$$\frac{R_{AB,CD} - R_{BC,DA}}{R_{AB,CD} + R_{BC,DA}} = f \operatorname{arcosh} \left\{ \frac{\exp(\ln 2 / f)}{2} \right\} \quad (2.17)$$

We can use Taylor expansion to estimate the function  $f$ .

$$f = 1 - \left( \frac{R_{AB,CD} - R_{BC,DA}}{R_{AB,CD} + R_{BC,DA}} \right)^2 \frac{\ln 2}{2} - \left( \frac{R_{AB,CD} - R_{BC,DA}}{R_{AB,CD} + R_{BC,DA}} \right)^4 \left\{ \frac{(\ln 2)^2}{4} - \frac{(\ln 2)^3}{12} \right\} + \dots \quad (2.18)$$

From the equation (2.18), apparently, if

$$f = 1, \text{ when } R_{AB,CD} = R_{BC,DA} \quad (2.19)$$

As the sample has a flat shape of uniform thickness and it is homogeneous and isotropic, we can say that  $R_{AB,CD} = R_{BC,DA}$ , so the function  $f$  should be 1. So (2.16) can be rewritten as

$$R_s = \frac{\pi R_{AB,CD}}{\ln 2} \quad (2.20)$$

As in fact  $R_{AB,CD}$  differs slightly from  $R_{BC,DA}$ , we always measure data for different directions and use the average of them to calculate the sheet resistance. The 8 data of the sample are

$$R_{AB,CD}, R_{BA,CD}, R_{CD,AB}, R_{DC,AB}, R_{BC,AD}, R_{CB,AD}, R_{AD,BC}, R_{DA,BC} \quad (2.21)$$

We use the average of these 8 data to calculate the sheet resistance. [3]

### 2.3.2.4 Measurement of Sheet Carrier Density and Mobility

Consider a sample shown in Fig 2.2, firstly we flow the current from contact A to contact C, while let the magnetic field be perpendicular to the surface of the sample, and measure the potential difference between contact B and contact D ( $V_D - V_B$ ). Then we reverse magnetic polarity, and measure the potential difference between contact B and contact D again. One of the two results of the measurement of the potential difference should be positive, and the other should be negative. Let us define the positive one,  $V_{AC-p}$ , because this potential difference is measured when the current flows from contact A to contact C. Likely, we can define the negative one  $V_{AC-n}$ . Then we define that

$$V_{AC} = V_{AC-p} - V_{AC-n} \quad (2.22)$$

Likely, we can have  $V_{CA}$ ,  $V_{BD}$  and  $V_{DB}$ .

The overall Hall voltage is

$$V_H = \frac{V_{AC} + V_{CA} + V_{BD} + V_{DB}}{8} \quad (2.23)$$

We can use this voltage to calculate the sheet carrier density like

$$n_s = \frac{IB}{qV} \quad (2.24)$$

We can calculate the mobility by the data of carrier density.

The resistivity can be written as

$$\rho = \frac{1}{q(n\mu_n + p\mu_p)} \quad (2.25)$$

When  $q$  is the charge on the particle,  $n$  is the concentration of negative carrier,  $p$  is the concentration of positive carrier, and  $\mu_n, \mu_p$  are the mobility of negative and positive carrier.

If we ignore the minority carrier, (2.25) can be written as

$$\rho = \frac{1}{qn_m\mu_m} \quad (2.26)$$

$n_m$  is the concentration of majority carrier and  $\mu_m$  is the mobility of majority carrier.

We can use sheet carrier density  $n_s$  and sheet resistance  $R_s$  to rewrite (2.26)

$$R_s = \frac{1}{qn_s\mu_m} \quad (2.27)$$

Hence

$$\mu_m = \frac{1}{R_sqn_s} \quad (2.28)$$

As sheet resistance  $R_s$  can be obtained by (2.27), we can calculate the mobility by using (2.28).

### 2.3.3 Equipment for Hall Effect

The equipment used for Hall Effect is shown in Fig 2.5 and Fig 2.6. Fig 2.5 is the equipment for Hall Effect at high temperature (Room Temperature~900K) and low temperature (80K~Room Temperature). Liquid Nitrogen is used in the Hall Effect measurement at low temperature to lower the temperature.



**Fig 2.5 Equipment for Hall Measurement at Low Temperature**



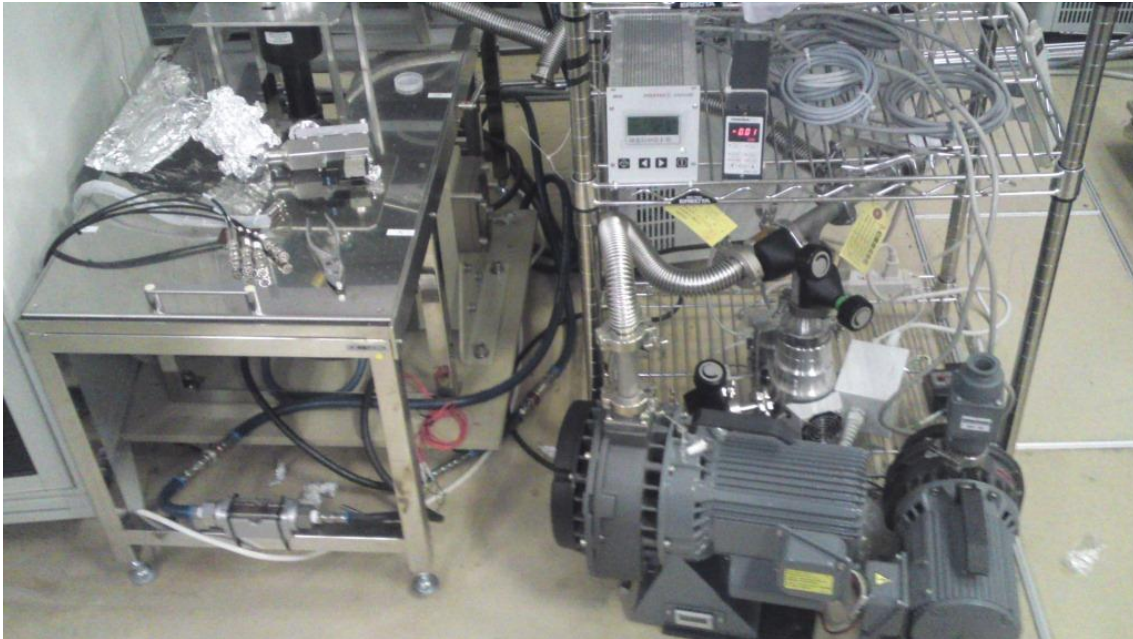


**Fig 2.6 Equipment for Hall Measurement at High Temperature**

## **2.4 Rapid Thermal Annealing (RTA)**

Rapid thermal annealing (RTA) is a piece of equipment used for heat treatment. Using the equipment shown in Fig 2.7 sample can be annealed in different atmosphere, to heal the crystal structure of the wafer. A great advantage of the RTA equipment is that temperature can fall and rise rapidly. The temperature change of 1000°C can be achieved in about 10-20 seconds. Due to the short processing time, the further diffusion of the dopants can be limited to a minimum.



**Fig 2.7 Equipment for Rapid Thermal Annealing**

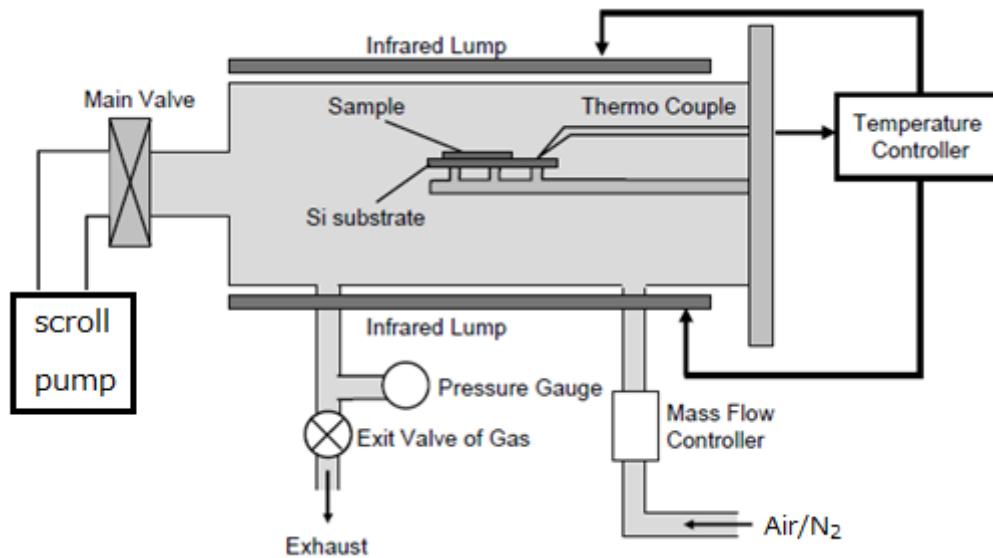


**Fig 2.8 Rapid Thermal Annealing**

As shown in Fig 2.8, the sample is under heat treatment in atmosphere in  $N_2 / O_2$  (8:2) gas, and  $N_2$  gas is used to surge pressure. [4]

## 2.5 Probe Station

The probe station is a machine used to acquire the signals from a semiconductor device.

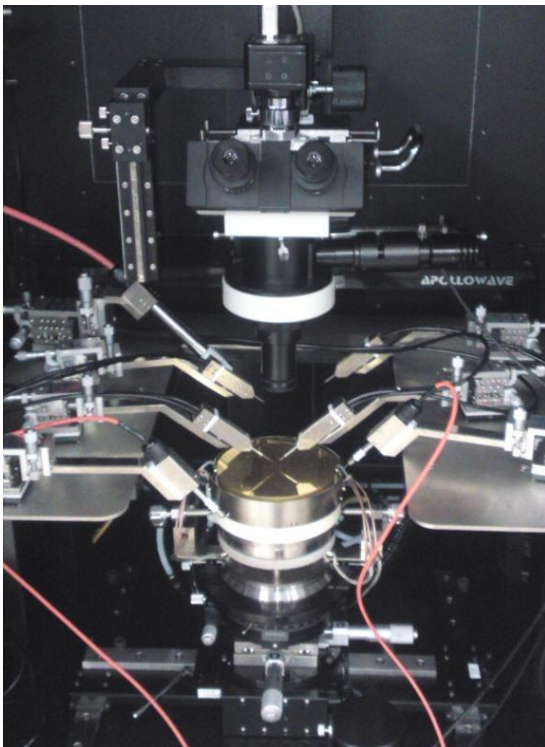


**Fig 2.9 Probe Station**

The total view of probe station is shown in Fig 2.9. The microscope is used to observe the sample and the location of the sample and probes. The probes can be controlled to contact the electrodes in the sample and obtain signals from the sample.

The image of the part of plate under the microscope is shown in Fig 2.10.

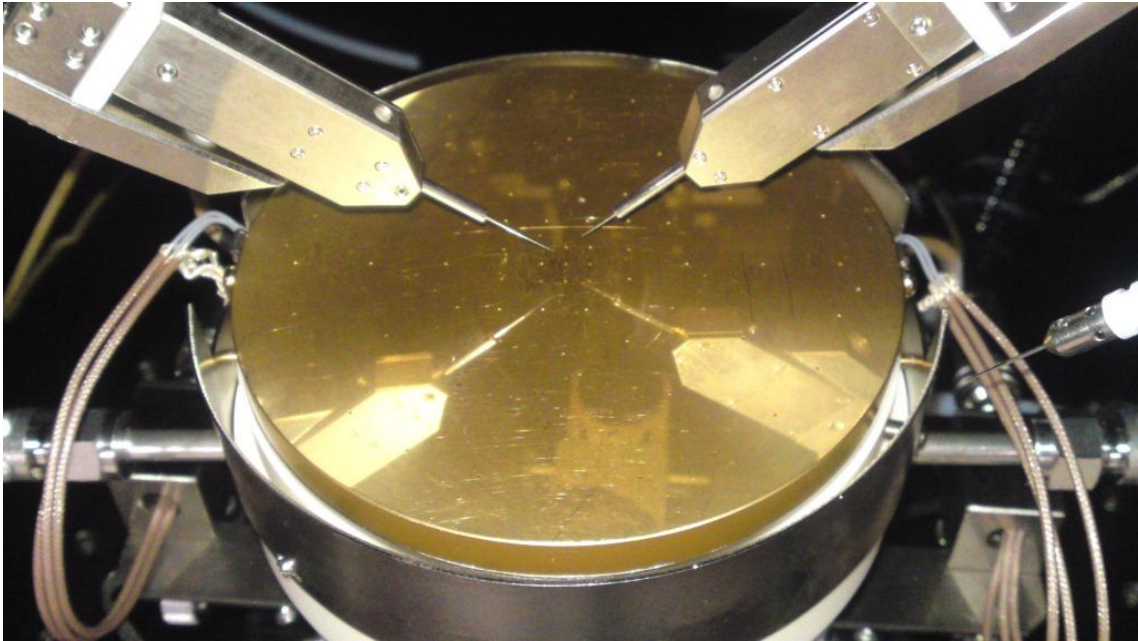


**Fig 2.10 Image of the Measurement Zone of Probe Station**

## **2.6 Photolithography**

Photolithography is a method using light-like material applied on the surface of a flat thin sample to produce particular pattern on the sample. The light-like material is called “resist”, and the light used in photolithography is usually ultraviolet (UV) light. The photolithography technique is used to produce metal contact to the surface of sample, which will be mentioned in Chapter 3.



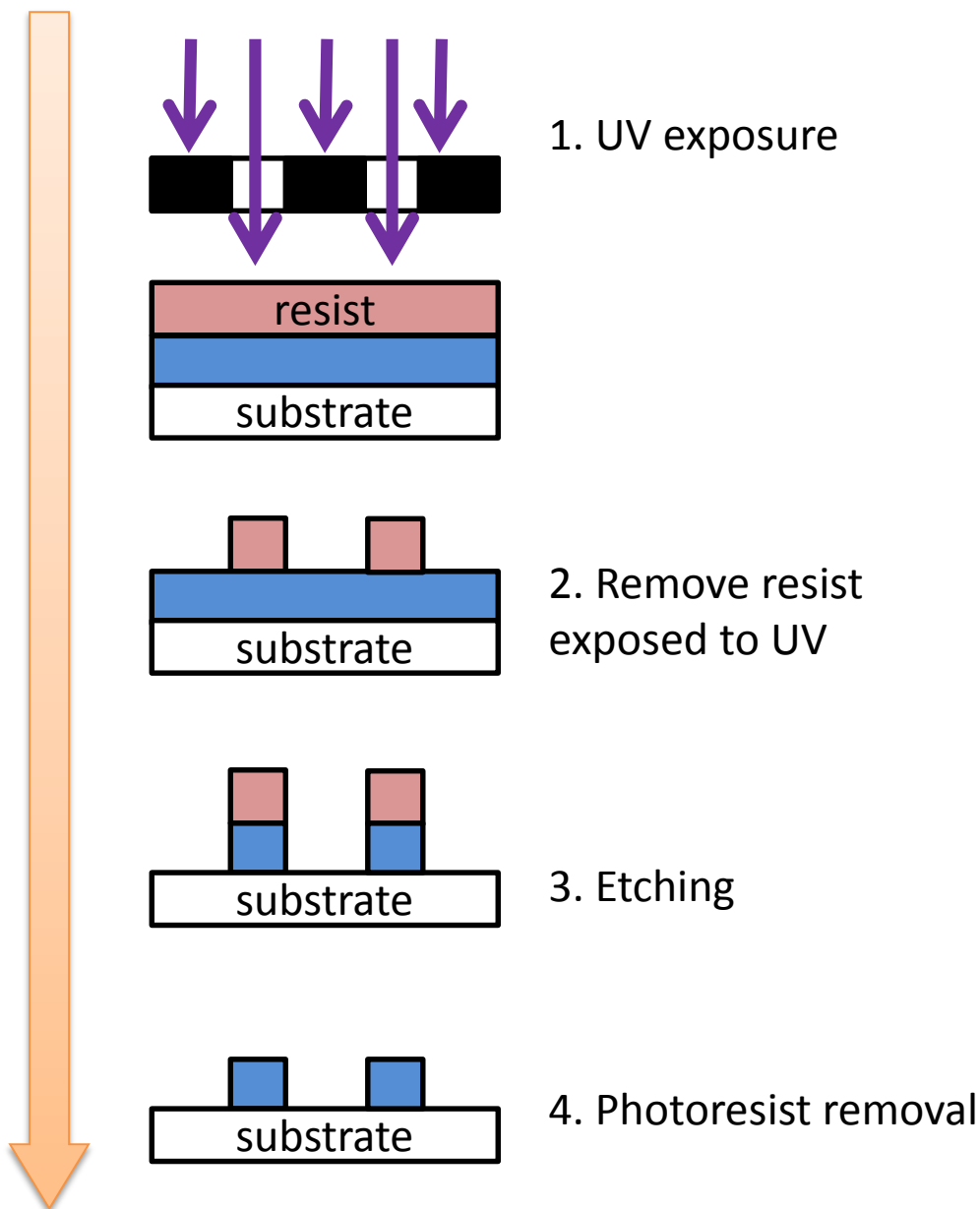


**Fig 2.11 Photolithograph Technique**

The process is shown as Fig 2.11:

- 1) Applying the resist to the sample. In the application, we usually use a machine call spin coater. A spin coater can rotate to high speed, and the sample can be placed on it. As the resist must be applied to the surface of the sample uniformly, we can use the centrifugal force to ensure it. First we apply the resist to the sample placed on the spin coater, and then rotate it to a high speed, and finally the resist will become a uniformly flat thin layer. After this, we should use a photomask which the light shines through but blocks light in some areas and lets it pass in others. The

photoresist is exposed to the UV light after aligning the photomask on the sample.

- 2) The exposure leads to a chemical change in resist. As a result, the exposed region and unexposed region become different chemically so the one of them can be removed by a special solution call photographic developer. Which one can be removed is depend on resist, and there are two kinds of resist: positive and negative. With positive photoresist, exposed regions are soluble in the developer. On the other hand, with negative photoresist, unexposed regions are soluble in the developer. The Fig 2.10 shows the situation of positive resist.
- 3) The region of upper layer to the substrate which is not protected by resist can be removed by some chemical materials in the process of etching. The chemical materials used in etching can be liquid or plasma.
- 4) After etching, the rest resist should be removed. A liquid call resist stripper can be used for the removal of resist. Another way to remove resist is ashing. In ashing a kind of plasma containing oxygen is used. The reactive species combines with the photoresist to form ash which is removed with a vacuum pump.

## Reference

- [1] Z.Tang, 1992, *Medicine Cell Biology*, Beijing Medical University Press
- [2] Y. Taur and Tak H.Ning, 2009, *Fundamental of Modern VLSI Devices*, 2<sup>nd</sup> edition, Cambridge Press
- [3] Van der Pauw, L.J, 1958, "A method of measuring specific resistivity and Hall effect of discs of arbitrary shape", *Philips Research Reports*, 13, 1–9
- [4] S.M.Sze, 1981, *Physics of Semiconductor Devices*, 1<sup>st</sup> edition, John Wiley & Sons, Inc.

## **Chapter 3: Experimental Procedures**

<b>3.1</b> Procedures Needed for the Research .....	29
<b>3.2</b> Preprocessing .....	29
<b>3.2.1</b> Methods for Preprocessing .....	29
<b>3.2.2</b> Most Suitable Method for Preprocessing .....	30
<b>3.3</b> Steps of Experiment .....	33
Reference .....	35

### 3.1 Procedures Needed for the Research

In this research, the GaN/AlGaIn heterostructure is produced in POWDEC Co., and what should be demonstrated is adding electrodes to the sample. As mentioned in section 2.3.2.2, proper heat treatment is necessary to lower the Schottky Barrier Height. Should it exist, the signal from the sample would not be properly obtained. Also, the state of the surface is importance, and proper preprocessing method is regarded fatal in experiment.

### 3.2 Preprocessing

In the manufacture process, preprocessing of the substrate by using different chemical materials is basic step. By treating the substrate with proper chemicals, the pollutant and compound such as oxide at the surface can be cleaned so the substrate can satisfy the requirement for next processing steps. And for many kinds of semiconductor elements, the more important reason is that the flat and clean surface can lead to an ohmic contact rather than Schottky contact between the semiconductor and metal contact to be added on, and it also affects the sheet resistance.

#### 3.2.1 Methods for Preprocessing

In the manufacture process, preprocessing of the substrate by using different chemical materials is basic step. By treating the substrate with proper chemicals, the pollutant and compound such as oxide at the surface can be cleaned so the substrate can satisfy the requirement for next processing steps. And for many kinds of semiconductor elements, the more important reason is that the flat and clean surface can lead to an ohmic contact rather than Schottky contact between the semiconductor and metal contact to be added on, and it also affects the sheet resistance.

Several methods of preprocessing on the GaN have been developed. Y.Koide *et al.* reported a sheet resistance of about  $2\sim 3 \times 10^{-3} \Omega\text{cm}^2$  by dipping in HF solution buffered with  $\text{HF}_2\text{NH}_4$  after immersing in acetone and isopropyl [1]. H.W.Jang *et al.* reported a sheet resistance of  $1.2 \times 10^{-4} \Omega\text{cm}^2$  by dipping in HCl solution (HCl:H<sub>2</sub>O=3:1) after  $\text{Cl}_2/\text{BCl}_3$  etching [2]. J-K.Ho *et al.* reported a sheet resistance of about  $4 \times 10^{-6} \Omega\text{cm}^2$  by etching with HCl solution (HCl:H<sub>2</sub>O=1:1) at room temperature for 1 minute [3]. There are some other reports about the preprocessing but without the objective data of sheet resistance. R.Wenzel *et al.* researched on several methods of preprocessing, and found that following is the best among which are tested: Firstly dip in acetone for 30 seconds, and then dip in 40% HF for 8 minutes and 65%  $\text{HNO}_3$  for 1 minute, and finally rinse in isopropanol for 30 seconds [4]. J-L.Yang *et al.* reported a preprocessing method using

alkali [5].

Considering the results of these reports and the equipment and chemicals on hand, we designed three methods for the preprocessing.

(a) HCl

In this experiment, a hydrochloric acid solution (volume ratio HCl:H<sub>2</sub>O=1:1) is used. It is mixed of 30cc HCl and 30cc ultra-pure water. The HCl liquid has not so strong oxidizing properties, but pollutants like oxide will dissolve in hydrochloric acid. The sample is placed in it for 60 seconds at room temperature. Then the sample is rinsed in the ultra-pure water for 1 minute.

(b) SPM

SPM is abbreviation for Sulfuric acid-Hydrogen Peroxide Mixture. This liquid is made of 15cc ultra-pure water, 15cc hydrogen peroxide and 45cc sulfuric acid. It has strong oxidizing properties and it is used for cleaning the pollutant of metal particles and organics at the surface. We place the sample in the SPM and use a hot plate to heat it. The temperature of the hot plate is set as 250 °C, and the temperature of the SPM liquid should to heated to 160~180 °C. The heating continues in 10 minutes. Then the sample is rinsed in the ultra-pure water for 1 minute after cooling to room temperature.

(c) HF

Hydrogen fluoride solution (40%) is used in this experiment. It is made of 10cc HF (50%) and 15cc ultra-pure water. It is also used for dissolving the pollutants like oxide at the surface. The sample is placed in it for 60 seconds at room temperature. Then the sample is rinsed in the ultra-pure water for 1 minute.

### 3.2.2 Most Suitable Method for Preprocessing

In order to find the best way for preprocessing, we conducted an experiment, which steps are shown in Fig 3.1. We produced three kinds of samples by different methods mentioned before to test. Firstly we performed organic solvent cleaning by acetone for 30 seconds and blowed the samples by gas gun, and then the preprocessing on the surface by the three methods: a) HCl; b) SPM; c) HF. After this the metal was added to the samples. The metal is 20nm nickel and 20nm gold. And the three kinds of samples were performed heat treatment in RTA. At first, it was set to 450 °C and continued 10 minutes. Then I-V property of the sample was measured in the probe station, and after it the sample was performed heat treatment again but in 500 °C. The process was conducted like this in also 550 °C and 600 °C.

The probe station is a machine used to acquire the signals from the sample. We obtained the current-voltage relationship of the two contacts in a diagonal line, so as there

are four contacts in a sample, we can have two I-V curves for each sample in each RTA temperatures.

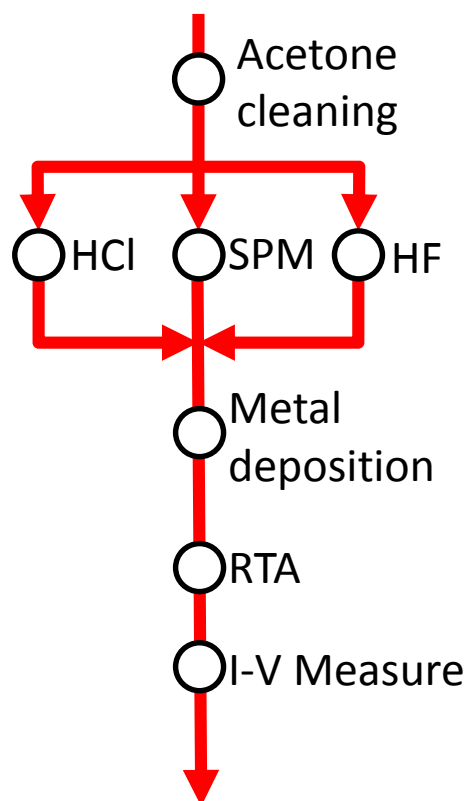


**Fig 3.1 Experiment of Preprocessing**

The result of the I-V measurement by the probe station is shown schematically in Fig 3.2, Fig 3.3, and Fig 3.4.

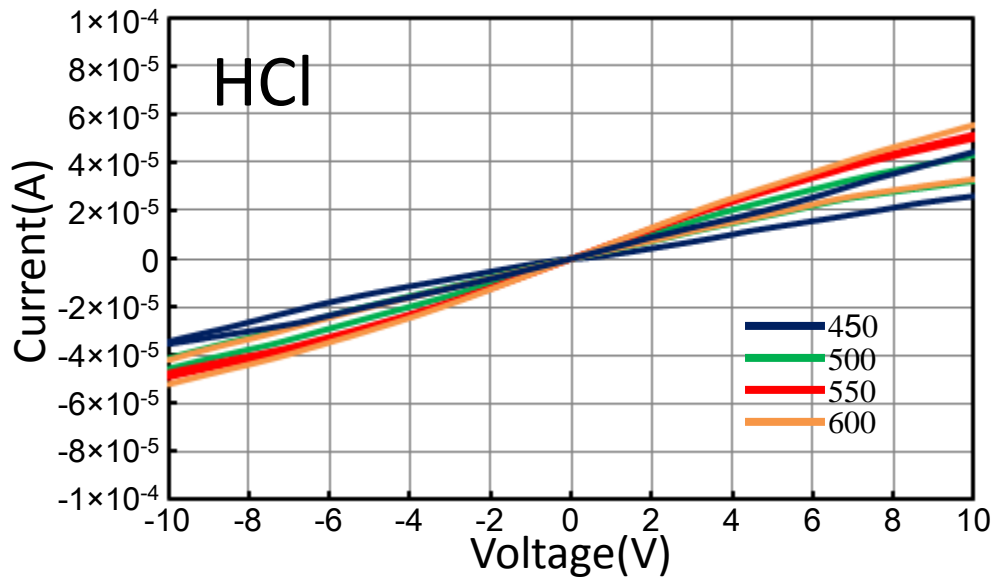


Figure 3.2 Measured V-I Current under Processing Condition (a)

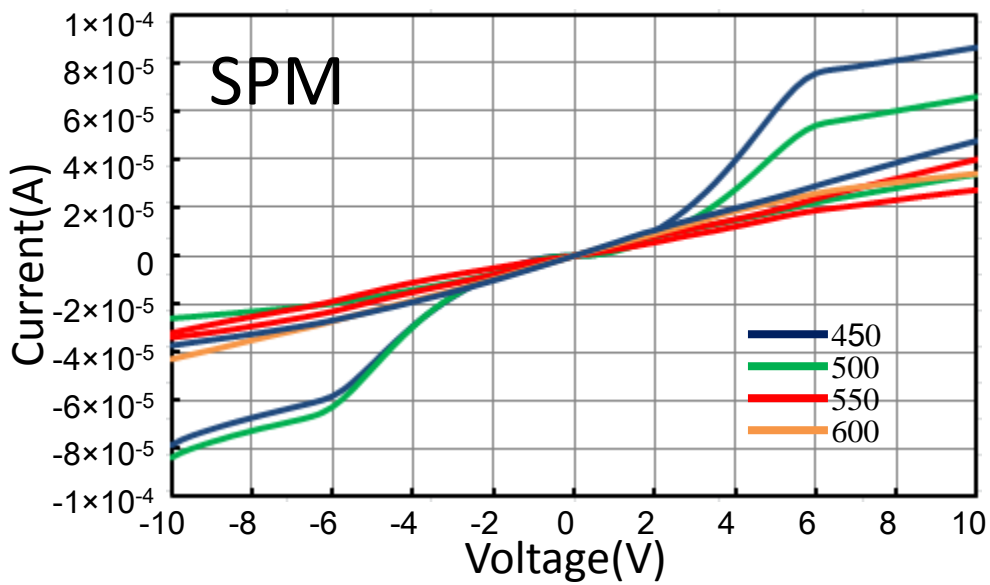
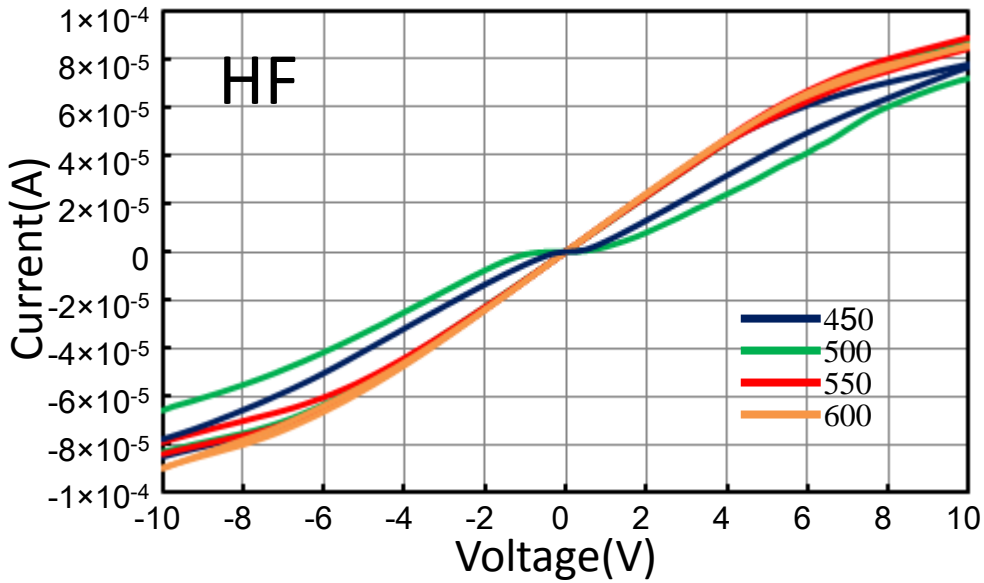


Figure 3.3 Measured V-I Current under Processing Condition (b)





**Figure 3.4 Measured V-I Current under Processing Condition (c)**

Considering the results of the three kinds of preprocessing, we found that to (c) HF is the best way to preprocess, for it has both a relatively high current and non-rectifying property.

### 3.3 Steps of Experiment

After deciding the method used in preprocessing, the experiment for adding electrode to the sample was demonstrated.

The steps of experiment are shown in Fig 3.5. Similar to the experiment in section 3.2.2, firstly organic solvent cleaning using acetone is performed, and then the sample is blowed the samples by gas gun. After this, the sample is place in Hydrogen fluoride solution (40%) for 1 minute. Then nickel 20nm and Au 20nm is added as electrode to the sample. After heat treatment in RTA for 10 minutes at 550°C in air atmosphere (N<sub>2</sub>:O<sub>2</sub>=8:2), Titanium 20nm and gold 100nm is added to the sample.

In the step of metal deposition, at beginning the method of lithograph which is was

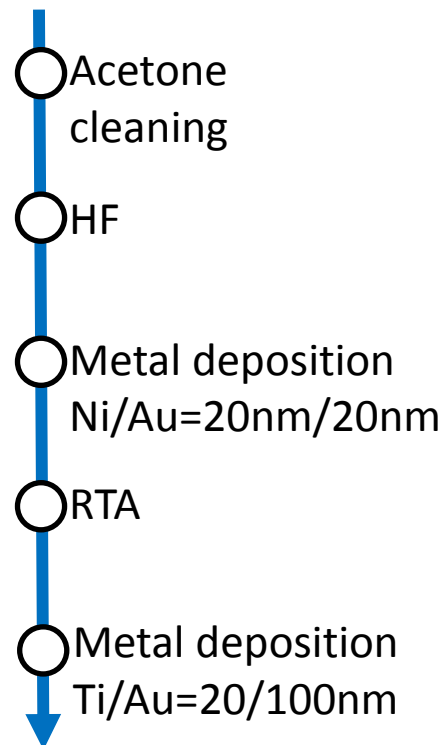


**Fig 3.5 Steps of Experiment**

mentioned in Chapter 2 has been tested, but we found that the ashing, which is used to remove the photoresist from the sample, is not so good, especially in lowering the Schottky Barrier Height.

Inside of the lithograph, we use a metal mask to deposit the metal to the surface of sample. The metal mask is a plate made of metal and there are small holes which is 0.3mm in diameter and equal to the diameter of metal electrode of the experimental producers in the plate. The steps of adding electrodes to the sample is shown schematically in the Fig 3.6,

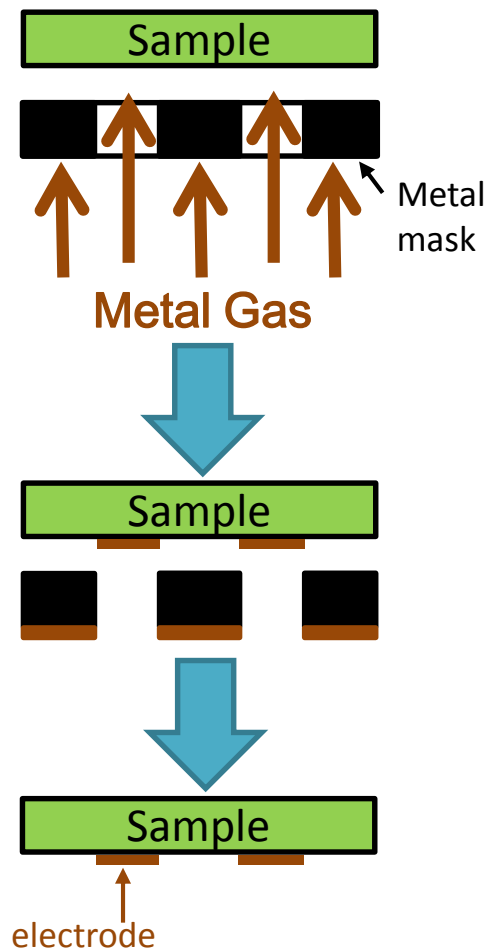


**Figure 3.6 Steps of Adding Electrodes to the Sample**

## Reference

- [1] Y.Koide, T.Maeda, T.kawakami, S.Fujita, T.Uemura, N.Shibata, and M.Murakami, 1999, “Effects of Annealing in an Oxygen Ambient on Electrical Properties of Ohmic Contacts to p-Type GaN”, *Journal of Electronic Materials*, **28**(3): 341-346
- [2] H.W.Jang, S.Y.Kim, and J-L.Lee, 2003, “Mechanism for Ohmic contact formation of oxidized Ni/Au on p-type GaN”, *Journal of Applied Physics*, **94**(3), 1748-1572
- [3] J-K.Ho, C-S.Jong, C.C.Chiu, C-N.Huang K-K.Shih, L-C.Chen, F-R.Chen and J-J.Kai, 1999, “Low-resistance ohmic contacts to p-type GaN achieved by the oxidation of Ni/Au films”, *Journal of Applied Physics*, **86**(8), 4491-4497
- [4] R.Wenzel, G.G.Fischer, R.Schmid-Fetzer, 2001, “Ohmic contacts on p-GaN (Part II): impact of semiconductor fabrication and surface treatment”, *Mterial Science in Semiconductor Processing*, **4**, 361-371
- [5] J-L.Yang, and J.S.Chen, 2006, “Effect of Ga dissolution in Au of Ni-Au system on ohmic contact formation to p-type GaN”, *Journal of Alloys and Compounds*, **419**, 312-318

## **Chapter 4: Results**

<b>4.1 TEM</b> .....	37
<b>4.2 SIMS</b> .....	38
<b>4.3 Dependence of sheet carrier density, sheet resistance and mobility on temperature</b> .....	39

## 4.1 TEM

The GaN/AlGaIn/GaN layer structure was observed in TEM, and we obtain the image of the heterostructure shown schematically.

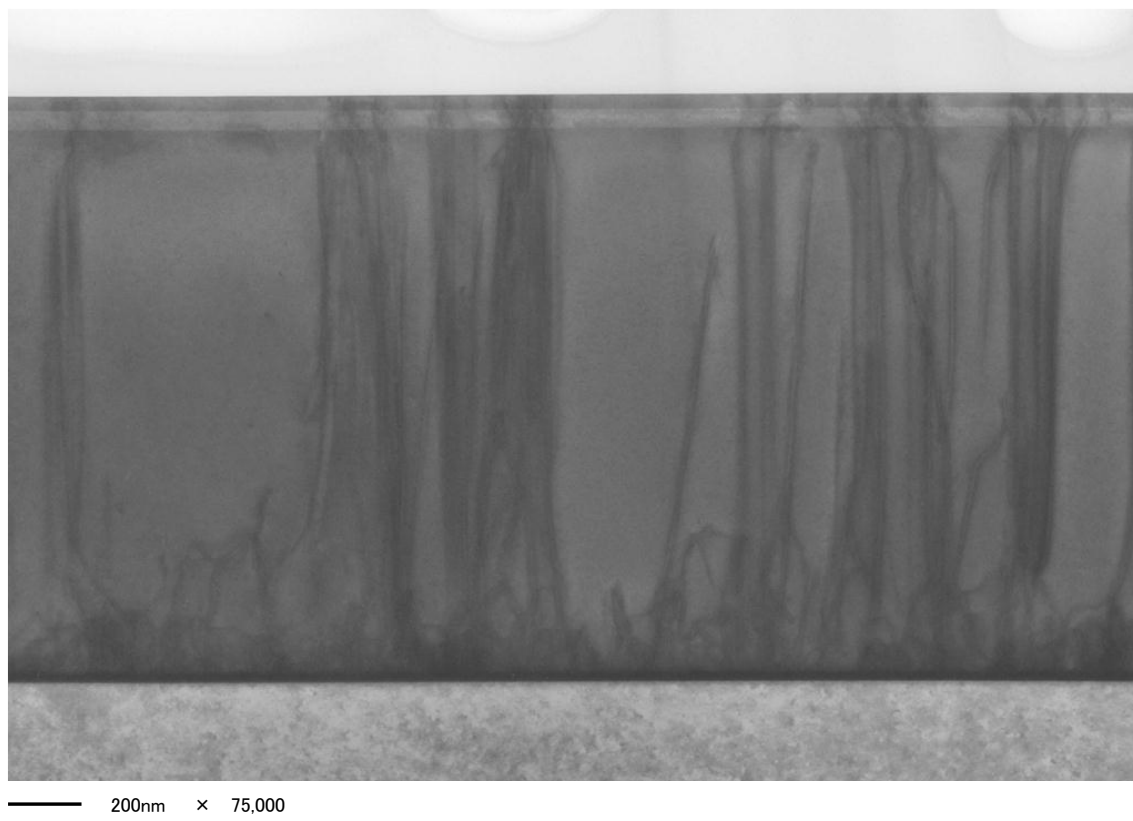


**Fig 4.1 The TEM Image of the GaN/AlGaIn/GaN Layer Structure**

In Fig 4.1, we confirmed the existence of three layers, and the depth of each layer was measured through the enlarged view of the upper surface shown at Fig 4.2, then the measurement result is shown in Fig 4.3. The measured depth of the layers approaches to the designed. Though the interface of Mg doped GaN and undoped GaN is not clear, the total depth of the layers of Mg doped GaN and undoped GaN can be confirmed in this image.

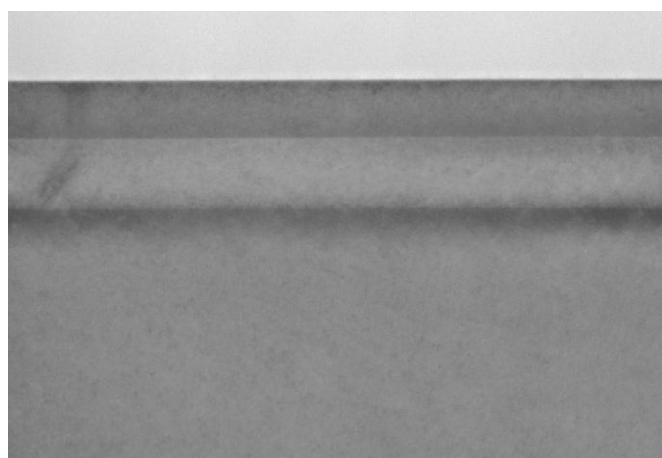


**Fig 4.2 Enlarged View of the Upper Surface of the GaN/AlGaIn/GaN Layer Structure**

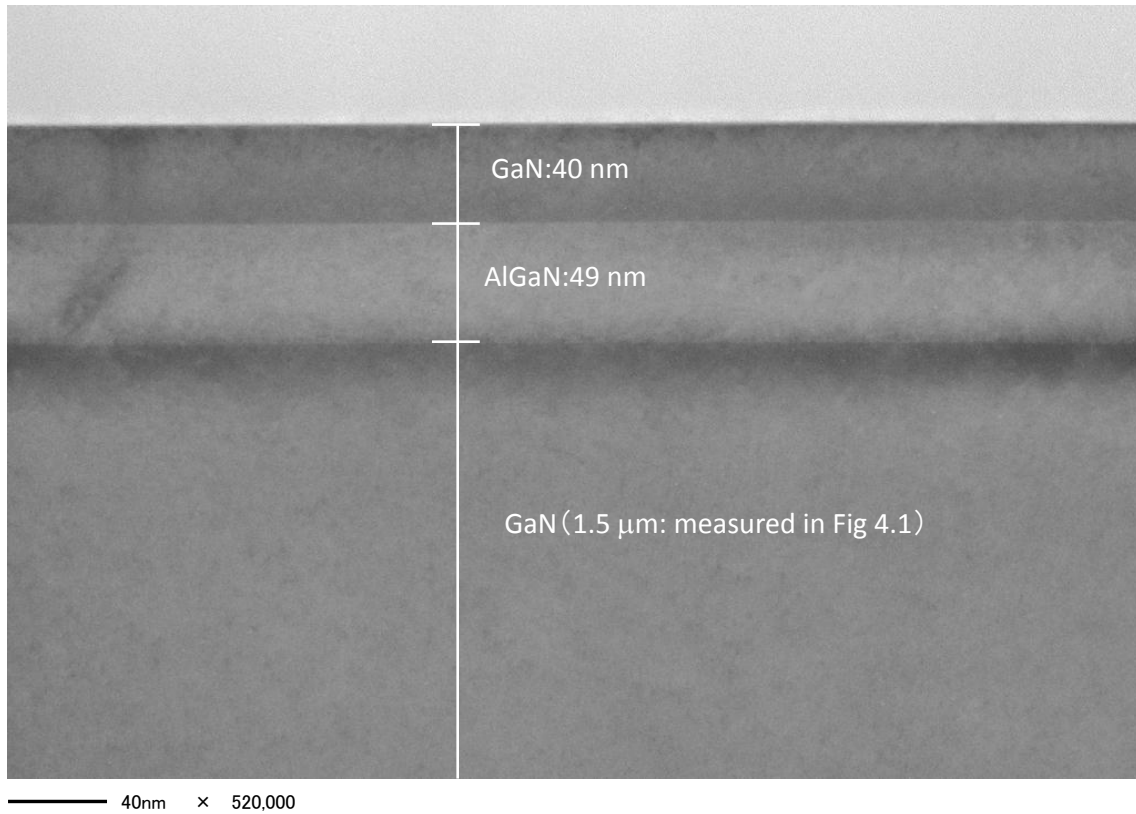


**Fig 4.3 Depth Measurement of SIMS Image**

## 4.2 SIMS

SIMS is used to analyse the concentration of the atoms. The concentration of Al, Mg, CsN and CsCa in depth of 0~400nm is shown schematically in Fig 4.3. We confirmed a concentration of  $4 \times 10^{21}$  atoms/cc of Al in the layer of AlGaIn.

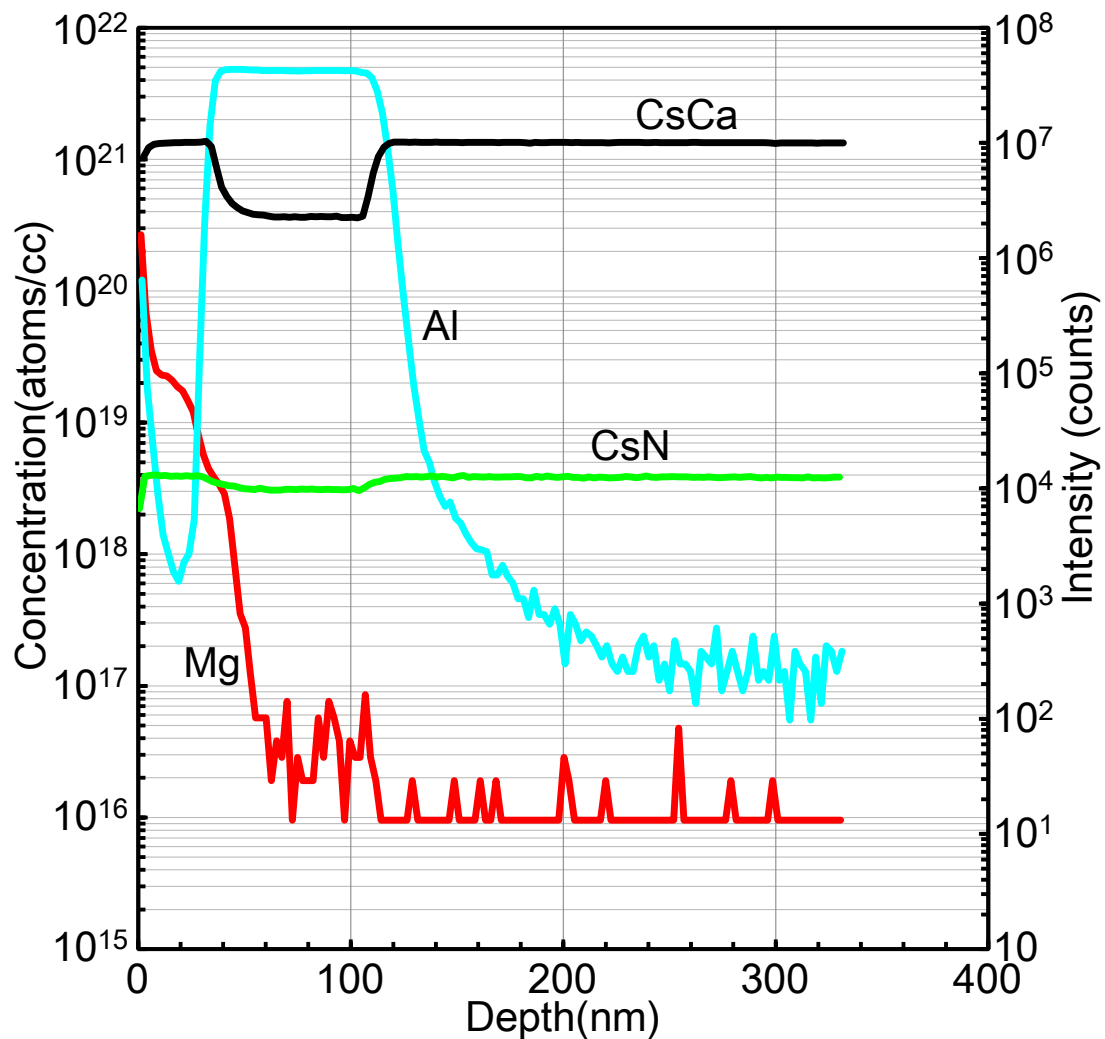


Fig 4.3 Analyses of Al, C, O and GaN by SIMS

### 4.3 Dependence of sheet carrier density, sheet resistance and mobility on temperature

Hall measurement by van der Pauw method is used in this research to obtain the relationship between sheet carrier density, sheet resistance, mobility and temperature. The structure we used in this measurement is shown in Fig 4.5 (b), as mentioned at the Chapter 1, and we also demonstrate the same Hall measurement on another sample shown in Fig 4.5 (a) as control. The graphs of the measurement results are shown schematically in Fig 4.6, Fig 4.7, and Fig 4.8.

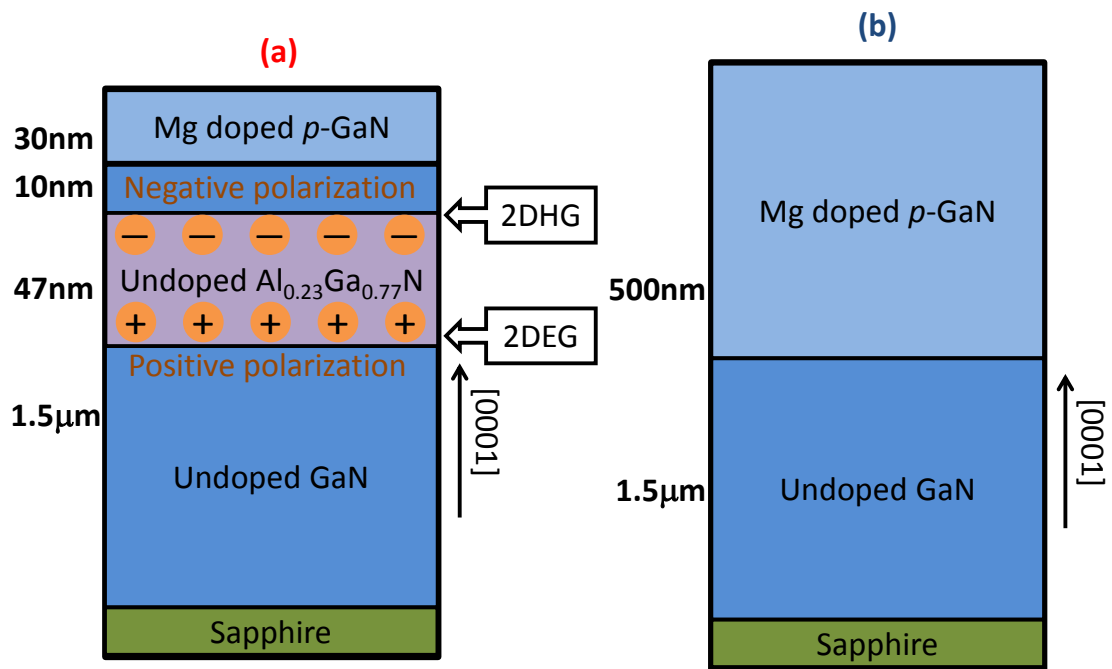


Fig 4.5 Structure of the Samples Used in the Hall Measurement

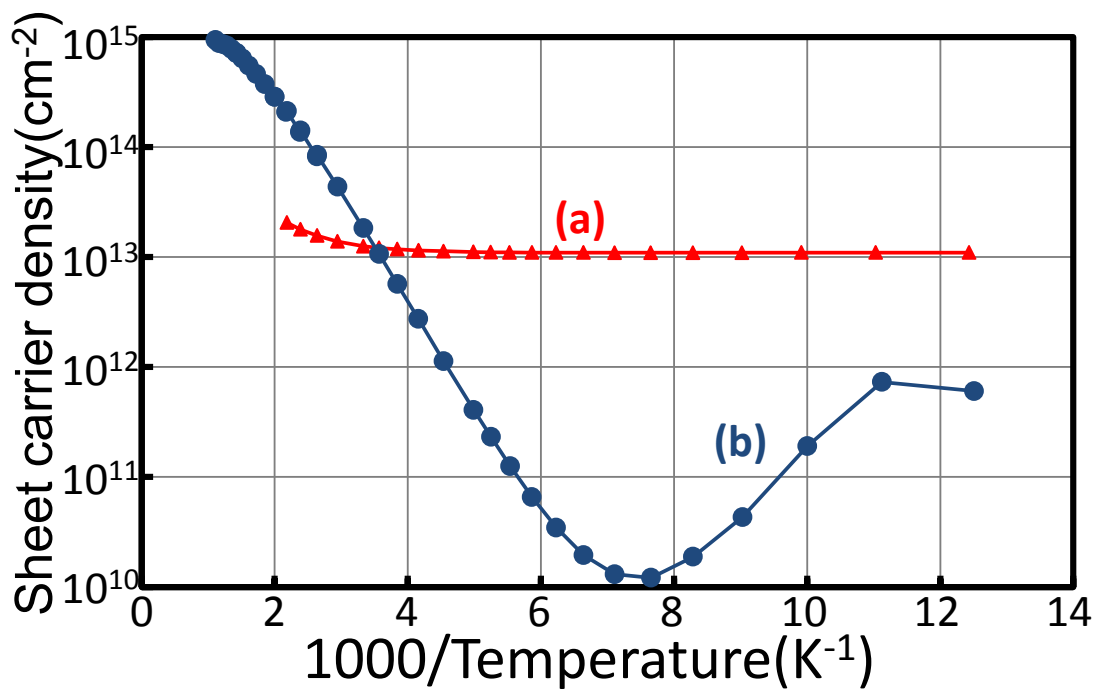


Fig 4.6 Sheet Carrier Density Dependence on Temperature



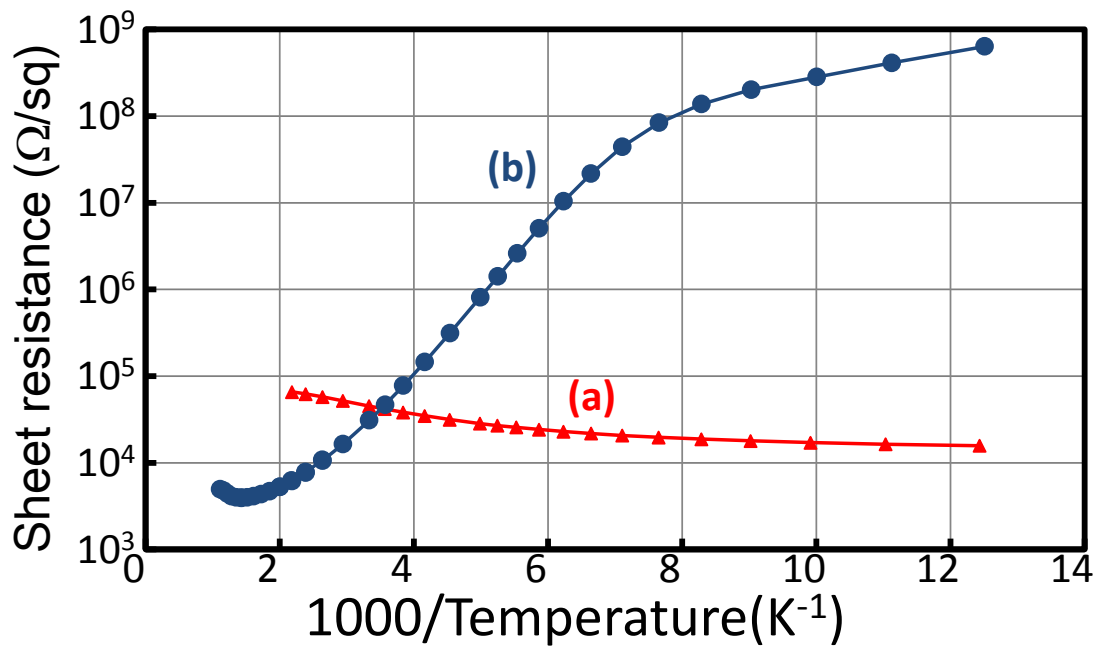


Fig 4.7 Sheet Resistance Dependence on Temperature

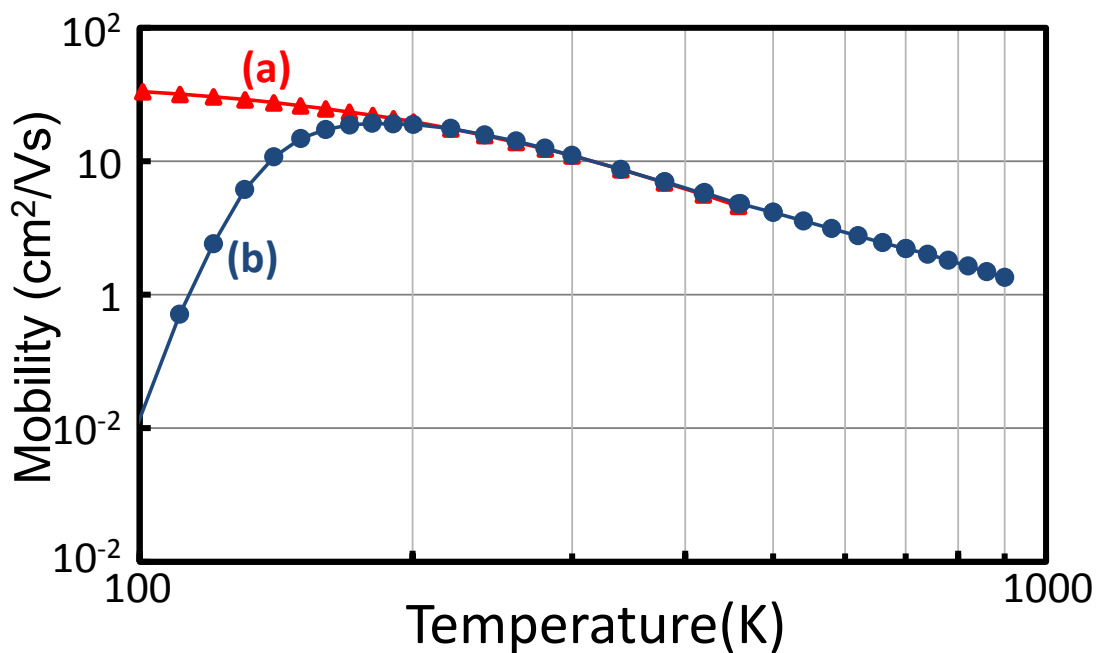


Fig 4.8 Mobility Dependence on Temperature

As shown in the graphs, the existence of the AlGaIn layer leads to a great change in electrical properties, and somehow it is certain that this kind of change owns to the 2DHG.

## **Chapter 5: Conclusion**

<b>5.1</b> Conduction Mechanism of Mg-doped GaN .....	43
<b>5.1.1</b> Band Conduction .....	43
<b>5.1.2</b> Impurity-band Conduction .....	47
<b>5.1.3</b> Hopping Conduction .....	47
<b>5.2</b> Conduction Mechanism of AlGa <sub>N</sub> /Ga <sub>N</sub> Heterointerface .....	48
Reference .....	50

## 5.1 Conduction Mechanism of Mg-doped GaN

### 5.1.1 Band Conduction

Band conduction is the most common and simple conduction seen in semiconductor. Shown schematically in Fig 5.1, 2 possible positions for electrons to exist are called valence band and conduction band. Between the valence band and conduction band, there is the band gap. Quantum mechanically, the electrons cannot exist in the band gap.

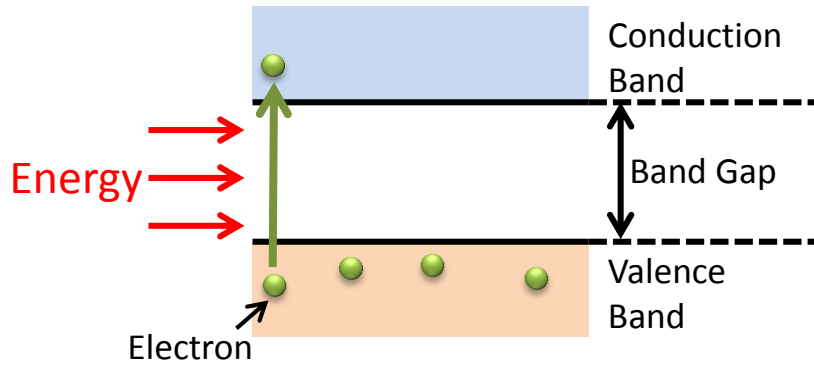


**Figure 5.1 Model of Band Conduction**

When the electrons in the valence band obtain some quantities of energy, which are at least equal to the energy of band gap, the electrons may move to the conduction band. The moving of the electron, which is usually called transition, leads to an important change for the electron. When the electrons exist in the valence band, as a part of the participators in the formation of a chemical bond, cannot move freely. It means that even electrons in the valence band are in an electric field, current will not be observed. But when the electrons transit to the conduction band, they can move freely and current will flow when electric field exists. It is same for holes, and in the next of this section, the situation of holes in  $p$ -type will be discussed.

Let  $n$  be electron density,  $N_A$  acceptor density,  $n_A$  unionized acceptor density,  $p$  hole density,  $N_D$  donor density, and  $n_D$  unionized donor density.

From electric neutrality,

$$n + N_A - n_A = p + N_D - n_D \quad (5.1)$$

and from (5.1),

$$p = n + N_A - n_A - N_D + n_D \quad (5.2)$$

For the situation of  $p$ -type is discussed,  $n$  and  $n_D$  can be ignored, so we have

$$p = N_A - N_D - n_A \quad (5.3)$$

$n_A$  satisfies the next equation (5.4)

$$n_A = \frac{N_A}{1 + \frac{1}{g} \exp\left(-\frac{E_A + E_F}{kT}\right)} \quad (5.4)$$

$g$  is for degeneracy.

By assuming  $p \ll N_V$ , hole density  $p$  and the carrier density of valence band  $N_V$  satisfy

$$p = N_V \exp[E_F/kT] \quad (5.5)$$

$E_F$  is for energy of Fermi level.

Then, let us identify a new variable  $N_V'$  to simply the calculation.

$$N_V' = \frac{N_V}{g} \exp[-E_A/kT] \quad (5.6)$$

From (5.4), (5.5), (5.6), we have

$$\begin{aligned} n_A &= \frac{N_A}{1 + \frac{\exp[-E_A/kT]}{g \cdot \exp[E_F/kT]}} = \frac{N_A}{1 + \frac{\exp[-E_A/kT]}{gp/N_V}} = \frac{N_A}{1 + \frac{N_V'}{p}} \\ &= \frac{N_A \cdot p}{p + N_V'} \end{aligned} \quad (5.7)$$

We can have  $N_V'$  from (5.3) and (5.7)

$$p = N_A - N_D - \frac{N_A \cdot p}{p + N_V'} \quad (5.8)$$

Hence

$$N_V' = \frac{p(p + N_D)}{N_A - N_D - p} \quad (5.9)$$

It is easy to have (5.10) from (5.6) and (5.9).

$$\frac{p(p + N_D)}{N_A - N_D - p} = \frac{N_V}{g} \exp\left(-\frac{E_A}{kT}\right) \quad (5.10)$$

The equation (5.10) is an important equation for analyzing the carrier density in semiconductor engineering. We use this equation to fit the result of sheet carrier density in section 4.3, but please pay attention that as the variables in (5.10) is all for carrier density rather than sheet carrier density, the result of carrier density calculated from sheet carrier density in section 4.3 is used here.

The figure is shown schematically in Fig 5.2.

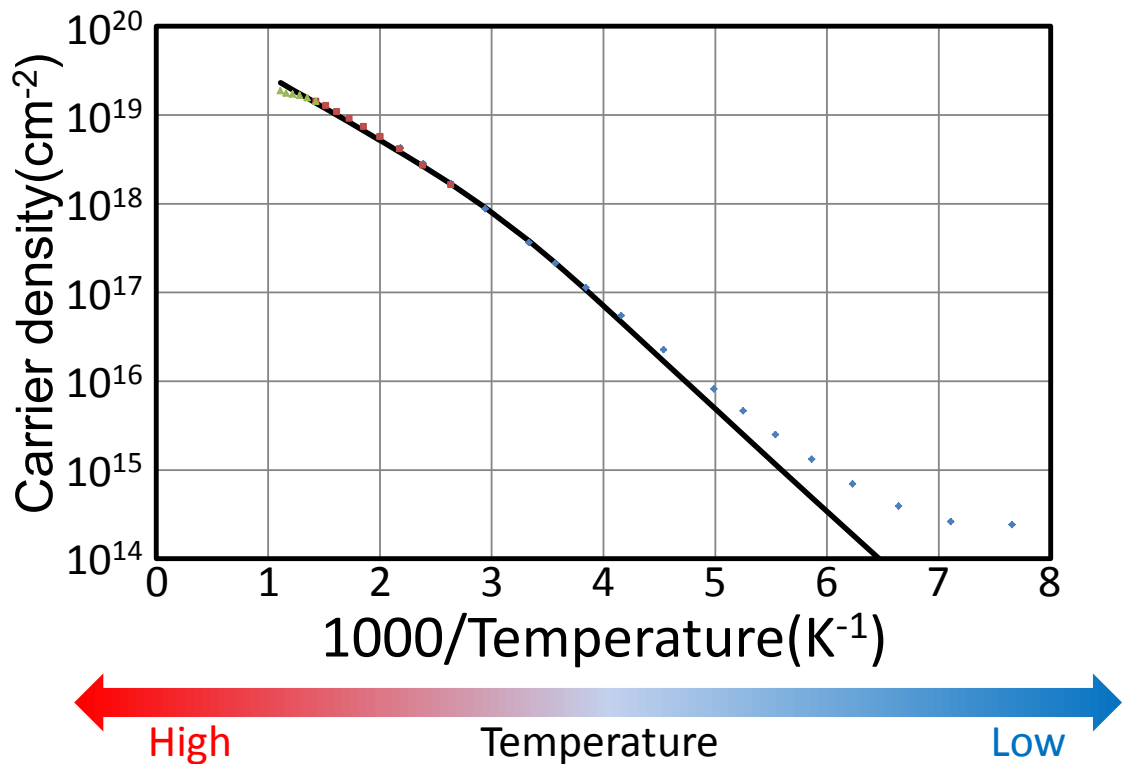


**Fig 5.2 Fitting Result of Carrier Density**

As shown in Fig 5.1, the black line stands for fitting, and the points stand for the experimental results. The horizontal axis is for  $1000/T$ , so the larger value means lower temperature. The red points, which are for the results at the temperature of 500K-700K, fit the theoretical value properly. The green points, which are for the results at a relatively high temperature of 700K-900K, show an error compared with the fitting results. The error in the high temperature could come from the assumption of Eq. (5.5) because hole density  $p$  is not negligible compare to effective density of state  $N_v$ . The blue points, which are for the results at temperature of 130K~500K, differ from the fitting results a lot, especially in low temperature of less than 200 K, though the results of lower temperature are not shown in Fig 5.2.

In the graph of sheet carrier density, a minimum value is found at about 130K, but the result of fitting shows us a monotonically decreasing function. This phenomena as reported in several articles, and generally impurity-band and hopping are considered as the main reasons. [1]

This fitting shows another important fact; that is the active acceptor is less than 1%, which is also reported in other articles.

### 5.1.2 Impurity-band Conduction

Impurity-band is a kind of energy band for carrier newly developed when the semiconductor is heavily doped. Hung *et al.* firstly reported this phenomenon when measuring resistivity using Hall Effect. [2,3,4] When the semiconductor is at low temperature, the impurity-band may become the main conduction instead of band conduction, and it is sometimes used to explain the unusual carrier density.

It is reported that in doped silicon and germanium, the conductivity follows that

$$\sigma = \sigma_3 \exp(-\varepsilon_3/kT) \quad (5.11)$$

Here  $\sigma_3$  is strongly dependent on the concentration of majority centres and  $\varepsilon_3$  is an order of magnitudes smaller than the energy required to ionize the center. [5] Whether such a theory is suitable for the situation of GaN or not is not clear, but at least we can confirm that it is a possible reason for the increasing carrier density while the temperature is decreasing at low temperature.

### 5.1.3 Hopping Conduction

Hopping conduction is another kind of conduction usually seen in organic semiconductors. The fitting of hopping conduction is shown in Fig 5.3. The detail is written below.

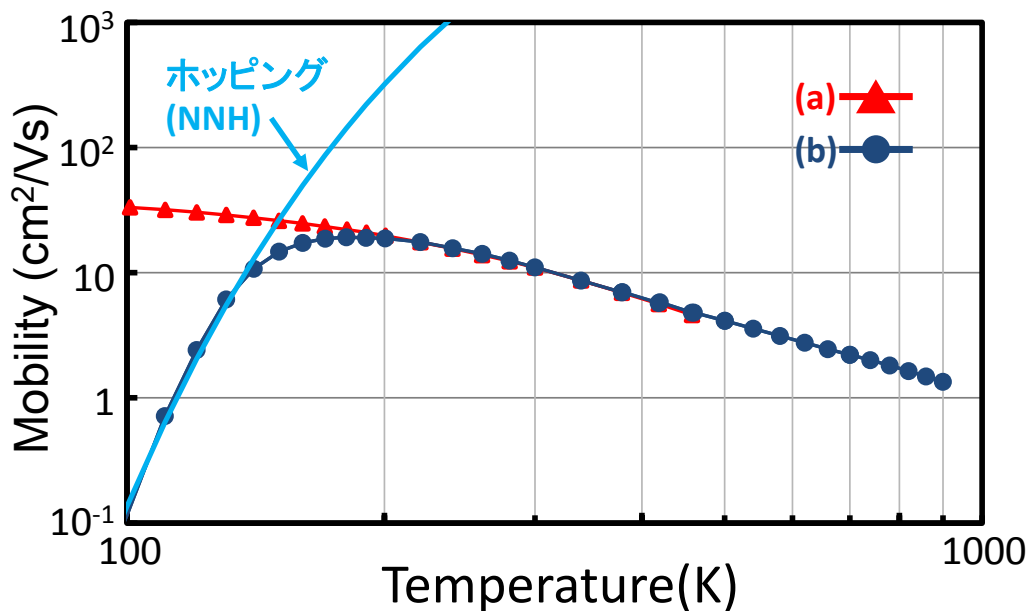


Fig 5.3 Fitting of Hopping Conduction

It is considered that, a quantity of carrier traps exist in the semiconductor material. When the carriers are near the carrier traps, the carrier may be trapped in the traps for the

carrier traps are potentially low. Once the carrier be trapped, the carriers can move out when obtaining enough energy. The possibility of the carrier to move out, is dependent to the energy they can obtain, and thermal energy is an important source. In account of this reason, it is clear that the mobility is lower when the temperature is lower.

Several models used to analyze the hopping conduction also prove this. For illustration, a model called nearest neighbor hopping, which is one of the most common used, shows us the mobility is

$$\mu_H = \frac{qR_H^2}{6kT} \exp(-2\alpha R_H) v_{ph} \exp\left(-\frac{W_H}{kT}\right) \quad (5.12)$$

This model also shows the negative dependence of temperature and mobility in hopping conduction. [6]

## 5.2 Conduction Mechanism of AlGa<sub>N</sub>/Ga<sub>N</sub> Heterointerface

Compared from the results in Chapter 4 with the Mg-doped GaN, the AlGa<sub>N</sub>/Ga<sub>N</sub> structure shows a constant property of carrier density. As the typical properties of Mg-doped GaN at low temperature are not observed in AlGa<sub>N</sub>/Ga<sub>N</sub> structure, it is likely that conduction mechanism of AlGa<sub>N</sub>/Ga<sub>N</sub> heterointerface structure is different from Mg-doped GaN.

Concretely speaking, the two characteristics in section 5.1, the increasing carrier density while the temperature decreasing at low temperature, and the increasing mobility while the temperature decreasing at low temperature, are not observed in AlGa<sub>N</sub>/Ga<sub>N</sub> heterointerface structure.

We conducted a fitting in the graph of mobility and the result is shown as Fig 5.4. Firstly the mobility at high temperature is fitted by the phonon scattering as (5.13).

$$\mu_{L2} \propto \left(\frac{m^*}{m_0}\right)^{-\frac{3}{2}} \cdot T^{-\frac{3}{2}} \left\{ \exp\left(\frac{\theta}{T}\right) - 1 \right\} \quad (5.13)$$

but only the phonon scattering cannot fit the result properly at low temperature, so we assume that there exists another scattering mechanism, so according to the Matthiessen's rule, the other scattering mechanism

$$\frac{1}{\mu_{(a)}} - \frac{1}{\mu_{phonon}} = \frac{1}{\mu_{add}} \quad (5.14)$$

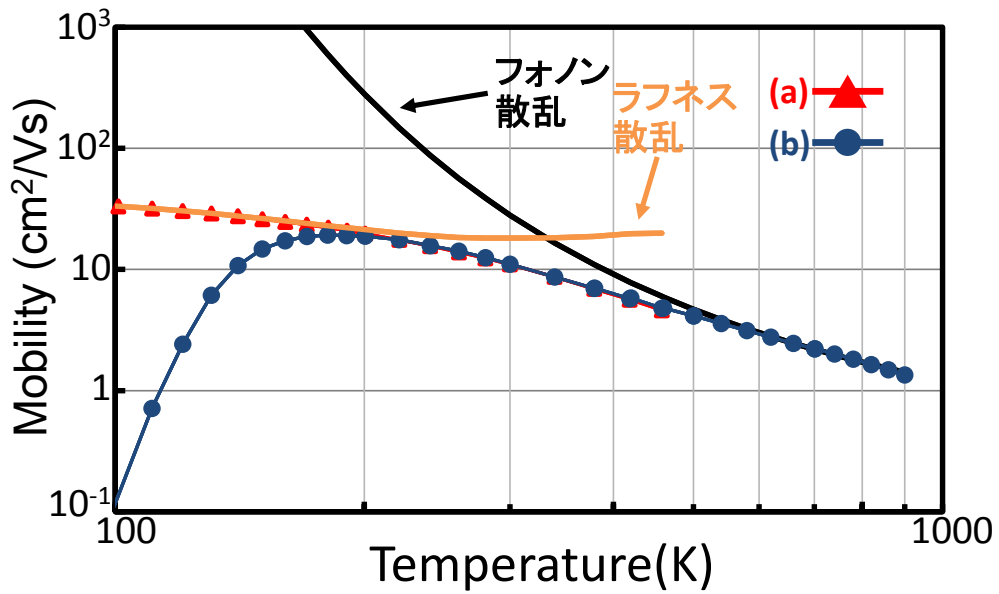


**Fig 5.4 Analysis of Scattering Mechanism**

The extra scattering shows independent property to the temperature, so a surface roughness scattering is considered possible. (Also, an alloy scattering in GaN/AlGaN heterostructure system is reported as  $10^3 \text{cm}^2/\text{Vs}$  and negligible in this situation [8])



## Reference

- [1] K.Kumakura, T.Makimoto and N.Kobayashi, 2003, “Mg-acceptor activation mechanism and transport characteristics in p-type InGaN grown by metalorganic vapor phase epitaxy”, *Journal of Applied Physics*, **93**(6), 3370-3375
- [2] C.S.Hung and J.R.Gliessman, 1950 “the resistivity and Hall Effect of germanium at low temperatures”, *Physical Review*, **79**, 729-730
- [3] C.Erginsoy, 1956, “On the Mechanism of Impurity Band Conduction in Semiconductors”, *Physics Review*, **80**, 1104-1105
- [4] S.Ohya, K.Takata and M.Tanaka, 2011, “Nearly non-magnetic valence band of the ferromagnetic semiconductor GaMnAs”, *Nature Physics*, **7**, 342-347
- [5] N.Mott, 1976, “Metal-Insulator Transition in an Impurity Band”, *Journal of Physics (Paris)*, **37**(10), 301-306
- [6] J.G. Simmons, 1967, “Poole-Frenkel Effect and Schottky Effect in Metal-Insulator-Metal Systems”, *Physical Review*, **155**, 657-660
- [7] R. Wittmann, 2007, “Miniaturization Problems in CMOS Technology: Investigation of Doping Profiles and Reliability”, Technischen Universität Wien Fakultät für Elektrotechnik und Informationstechnik
- [8] I. P. Smorchkova, L. Chen, T. Mates, L. Shen, S. Heikman, B. Moran, S. Keller, S. P. DenBaars, J. S. Speck, and U. K. Mishra, 2001, “AlN/GaN and (Al,Ga)N/AlN/GaN two-dimensional electron gas structures grown by plasma-assisted molecular-beam epitaxy”, *Journal of Applied Physics*, **90**(10), 5196-5201

# Acknowledgement

My deepest gratitude goes first and foremost to Professor Hiroshi Iwai and Assistant Professor Kuniyuki Kakushima, who are ones of the best professors that I have ever met. Without their instruction, this thesis could not have reached its present form.

I deeply thank to Dr. Akira Nakajima, researcher of National Institute of Advanced Industrial Science and Technology (AIST), for his devotedly help for this research. Also thank to Dr. Hiromichi Ohashi, Dr. Shin-ichi Nishizawa, Dr. Toshihara Makino, and Dr. Masahiko Ogura for their help and advice for this research.

I would also like to thank Professor Takeo Hattori, Professor Kenji Natori, Professor Nobuyuki Sugii, Professor Akira Nishiyama, Professor Yoshinori Kataoka, Professor Kazuo Tsutsui, and Associate Professor.

Parhat Ahmet, for their help in daily research life.

I also thank for the research colleges in Iwai Laboratory, for their friendship, and appreciate the support of Ms.Nishizawa and Ms.Matsumoto, the secretaries of Iwai Laboratory.

Besides, I want to say thanks to the other considering professors of Department of Electrical and Electronic Engineering of Tokyo Institute of Technology, for their help and advice for studying life during the 4 years. I also appreciate the professors in Foreigner Students Center of Tokyo Institute of Technology, for their every suggestion for me when I have problems as a foreigner student in Japan.

At last but not the least, I want to thank my parents, Liu Donghui and Chen Hui, for their support and encouragement.

Yokohama, Japan  
February, 2013

*[Domestic Presentation]*

The 60<sup>th</sup> Japan Applied Physics Society Spring Meeting, 2013, “Conduction Mechanism at Low Temperature of 2-Dimensional Hole Gas at GaN/AlGa<sub>N</sub> Heterointerface”, Kanagawa Institute of Technology

*[International Presentation]*

IEEE EDS WIMNACT 37: Future Trend of Nanodevices and Photonics, 2013, “Transport characteristics of 2 dimensional hole gas in AlGa<sub>N</sub>/GaN”, Tokyo Institute of Technology, Tokyo, Japan